2.1 Introduction

Nitrogen-containing heterocycles are the most popular structural components of pharmaceuticals and agrochemicals. More than 75% of drugs approved by the Food and drug administration (FDA) carry nitrogen heterocycles in their structures [1,2]. The number of novel *N*-heterocyclic moieties with significant physiological properties and promising applications in medicinal chemistry are ever-increasing [3-5]. Among the vast array of such compounds, tetrazole and their derivatives are particularly interesting and have been included in the top 25 most commonly utilized nitrogen heterocycles in pharmaceuticals. Tetrazoles are a class of synthetic aromatic heterocyclic compounds consisting of a five-membered ring with four nitrogen atoms and one carbon atom [3,6]. Depending on the number of substituents, tetrazoles are classified into four categories- (i) parent tetrazoles, (ii) monosubstituted tetrazoles, (iii) disubstituted tetrazoles, and (iv) trisubstituted tetrazolium salts (Figure **2.1**) [7,8].

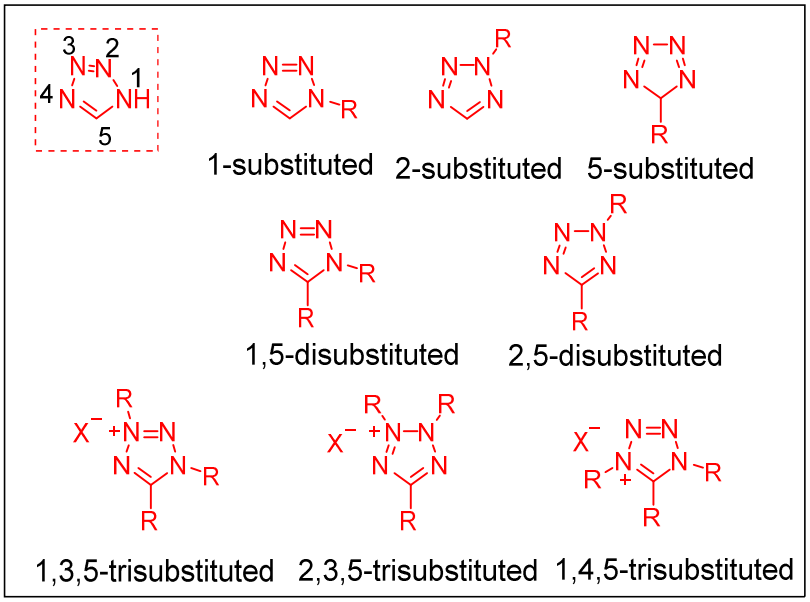

Figure **2.1** Classification of tetrazole scaffold

Tetrazoles contain free N–H bond which exists in two tautomeric forms; 1*H*-tautomer or 2*H*- tautomer of which the 1*H*- form is more stable and predominant in solution phase, whereas 2*H*- form is more stable in the gas phase (Scheme **2.1**) [9,10]. Due to their high stability to various oxidizing and reducing agents and also

to a wide range of pH, these compounds have widely been considered as a suitable precursor to various significant scaffolds [2,11].

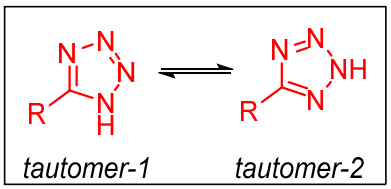

Scheme **2.1** Tautomerism in tetrazole derivatives

Tetrazole derivatives such as 1,5- and 2,5-disubstituted tetrazoles are used as carboxylic acid isosteres and amide isosteres due to their similar pK_a values which offers a preferable pharmacokinetic profile and a metabolically stable substitute for them [12]. Due to such attractive drug-like properties and metabolic stability, the incorporation of tetrazole moiety into drug molecules has gained interest among the scientific community [13-15]. There are numerous pharmacological applications of tetrazoles such as anti-inflammatory, antihypertensive, anticancer, anti-allergic, antibiotic, diuretics and receptor modulatory agents [16-18]. Some biphenyl-substituted tetrazoles like losartan, irbesartan which are important drugs of the sartan family having application in the synthesis of certain antihypertensive drugs (Figure **2.2**) [19,20]. Candesartan Cilexetil, an angiotensin II receptor blocker (ARB) drug is a 5-aryl-1*H*-tetrazole; whereas azosemide is a diuretic and pemirolast is an antiallergic drug (Figure **2.2**). Apart from these diverse pharmacological activities, they also offer a plethora of applications in the domain of coordination chemistry, material science, high energy materials, biochemistry and agriculture (as herbicides and fungicides) [21-24].

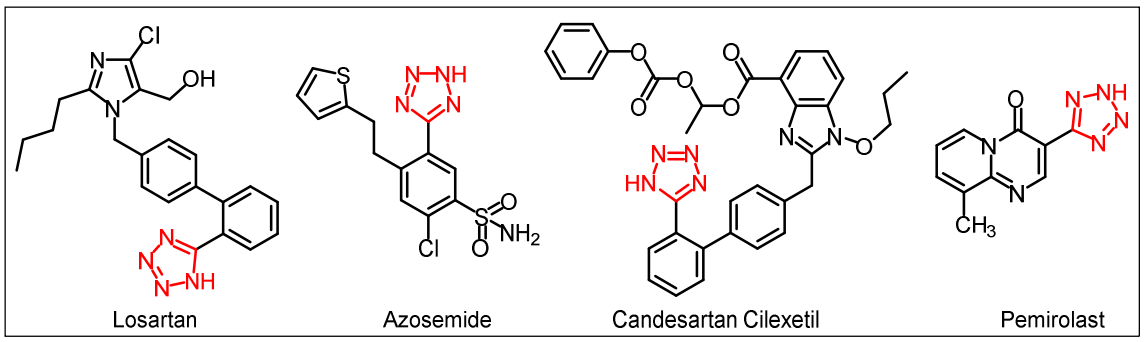

Figure **2.2** Selected drug molecules containing tetrazole moiety in their structure

2.1.1 Synthesis of tetrazoles

Tetrazole was first synthesized and characterized by the Swedish chemist, J. A. Bladin in 1885 at the University of Upsala [25,26]. However, the conventional methods of synthesizing tetrazoles are based on [3+2] cycloaddition strategy of azide ions to organic nitriles in the presence of a suitable catalyst. Majority of these catalysts are based on metals such as copper, iron, cadmium, palladium, aluminium, zinc, silver, titanium as well as lanthanide triflates. A number of the above mentioned methods for tetrazole preparation are in use, but some of these methods have potential limitations such as lower yields, drastic reaction conditions, use of expensive water sensitive reagents, toxic metal catalysts, tedious work-up, complex isolation and recovery procedures [27,28]. One of the first extensively used methods for the synthesis of 5-substituted-1*H*-tetrazoles before the [3+2] cycloaddition reaction consisted of the diazotization of amidrazones. These amidrazones were prepared from imidates and hydrazine. In this method, an imidoyl azide was formed prior to the formation of a 5-substituted-1*H*-tetrazole (Scheme **2.2, 1a**).

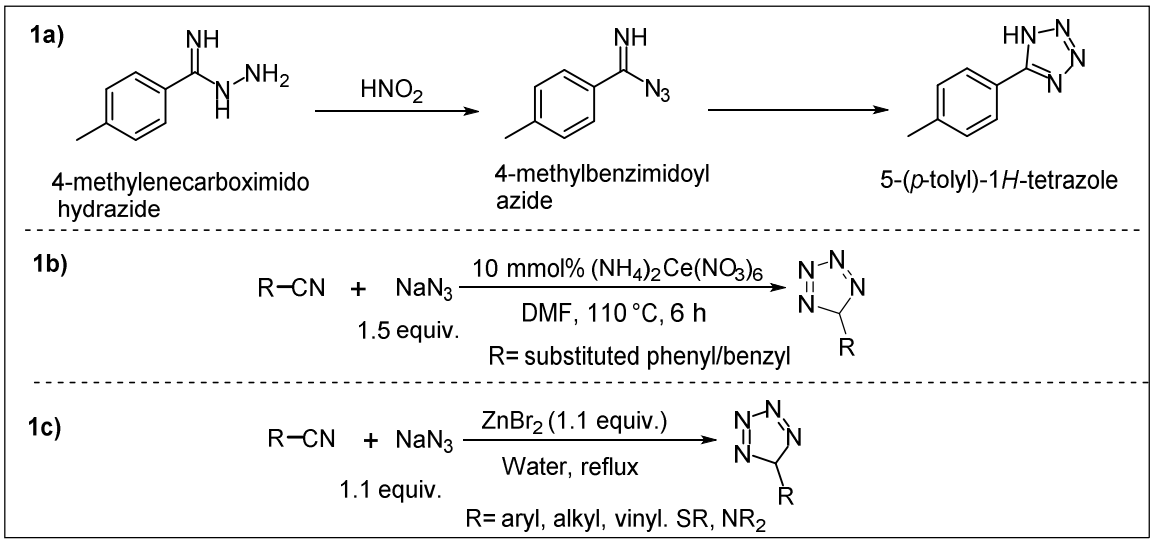

Scheme **2.2** Procedures for tetrazole synthesis

Among different procedures developed so far use of different organic nitriles with sodium azide and ceric ammonium nitrate (CAN) as catalyst for synthesis of 5-substituted-1*H*-tetrazoles is found to be superior. In an effort to develop a better catalytic system, the protocol was standardized and the optimized reaction conditions were represented by 1 mmol nitrile, 1.5 mmol NaN_3, and 10 mol% of

CAN in DMF at 110 °C (Scheme **2.2, 1b**) [29]. Another simple and high yielding protocol for transforming a wide variety of nitriles into the corresponding 1*H*-tetrazoles is by the addition of NaN_3 to nitriles in water in presence of zinc salts as catalysts (Scheme **2.2, 1c**) [30].

2.2 C–N cross-coupling

C–N bond formation remains as one of the most widely practiced reactions in synthetic chemistry due to its prevalence in a large number of natural products and pharmaceutically active compounds [31,32]. The development of transition metal (TM) catalysed methodologies affording new C–N bonds has been a pivotal step in the synthesis of organic molecules of biological interest. Considering the widespread importance of C–N bonds in organic materials, pharmaceutical compounds, and agricultural chemicals; the development of more efficient and convenient ways to form C–N bonds has become one of the hottest research goals in synthetic chemistry [33].

There are two main approaches towards TM-catalysed C–N bond formation: classical electrophile-nucleophile, by Buchwald-Hartwig and Ullmann-Goldberg reactions, and oxidative nucleophile–nucleophile, by Chan-Lam cross-coupling reaction (Scheme **2.3**) [12].

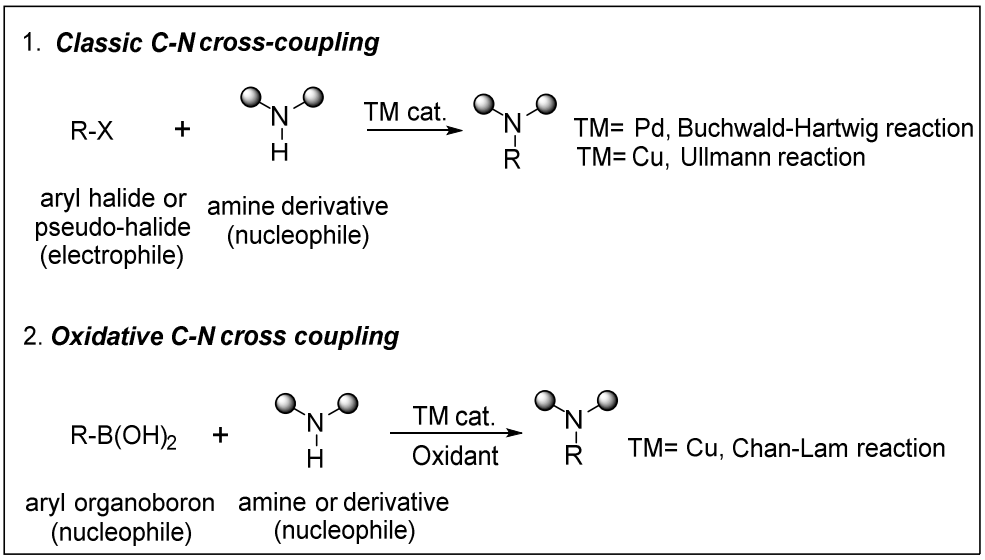

Scheme **2.3** General approaches to TM catalysed C–N cross-coupling

Earliest forms of Cu-catalysed C–N coupling reactions between *N*-nucleophiles and aryl halides are Ullmann and Goldberg reactions reported in 1903 and 1906, respectively [34]. It is not surprising that considering the boom in Cu-catalysed synthesis and the importance of carbon-heteroatom bonds, these reactions rapidly garnered attention and have been regarded as one of the major strategies for synthesizing heterocycles. Cu-catalysed methods offered versatility, such as inexpensive Cu source and mild reaction conditions [35]. However, to some extent, Ullmann coupling required harsh reaction conditions such as high temperature (typically > 200 °C), strong bases, stoichiometric amounts of metal catalyst, usage of toxic solvents and expensive ligands. Other methods for C–N bond formation has utilized *p*-tolyllead triacetate, *N*-metalated heterocycles (metal= Sn) and diaryliodonium salts as coupling partners which resulted in the generation of a large amount of toxic wastes such as organolead, organotin and aryliodides. Buchwald–Hartwig amination reaction, on the other hand, is catalysed by the expensive palladium catalyst [3,36,37].

2.2.1 Chan-Lam cross-coupling reaction

A breakthrough in nucleophile-nucleophile (oxidative) coupling was realized in 1998 with the discovery of the copper promoted Chan–Lam coupling reaction for the construction of C–N bond (Scheme **2.4**). Copper-mediated C–N, C–O and C–S bond formation between –OH, –NH, or –SH containing nucleophilic substrates and aryl- or alkenylboronic acids for the formation of the corresponding arylated or alkenylated products is referred to as the Chan–Lam cross-coupling reaction [38,39]. Compared to other coupling reactions Chan-Lam reactions featured several advantages:

i) The reaction employs convenient, inexpensive and readily available copper catalyst and costlier ligands are less utilized.
ii) “Open-flask” reaction condition i.e., ambient temperature, mild base and oxidant as open air are employed.
iii) The arylating partner i.e., organoboronic acids are easily accessible, stable or insensitive to moisture and allow reactions in aqueous medium.

iv) The reactions are compatible with a wide range of target nucleophiles and tolerate a broad range of sensitive functional groups.

The term CEL is used synonymously with Chan–Evans-Lam cross-coupling [38,40]. The mild reaction conditions concomitantly proposed by Chan, Lam and Evans for C–N and C–O bond formation significantly improved the possibility by allowing the coupling of arylboronic acids with various *N*- or *O*-nucleophiles [3,20]. Chan-Evans-Lam (CEL) cross-coupling is one of the most utilized C–N bond forming reactions and several novel drug molecules have been synthesized utilizing CEL cross-coupling methodologies in the synthetic route.

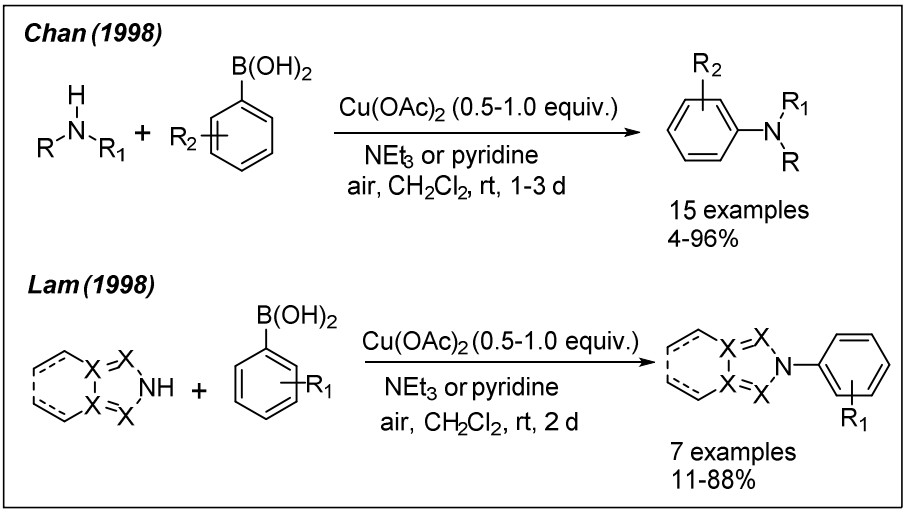

Scheme **2.4** Oxidative C–N bond formation reported by Chan and Lam

Lam and co-workers expanded the original scope of copper-mediated C–N bond formation, towards a variety of *N*-containing heterocycles such as imidazole, pyrazole, triazole, tetrazole, benzimidazole and indazole providing valuable *N*-arylated heterocycles. Thus CEL couplings have now been successfully employed for a large variety of *N*-, *O*-, *S*-, and even *C*-nucleophiles [41,42].

The arylating partners

The arylating partners in Chan-Lam cross-coupling reactions are the arylboronic acids and its derivatives. Lower toxicity, structural diversity, easy availability and moisture stability are the advantages of aryl boronic acids. From green chemistry context, they are regarded as “green” on account of their ultimate degradation to

boric acid. Varied boronic acids used in Chan-Lam cross-coupling reactions are depicted below (Figure **2.3**) [43,44].

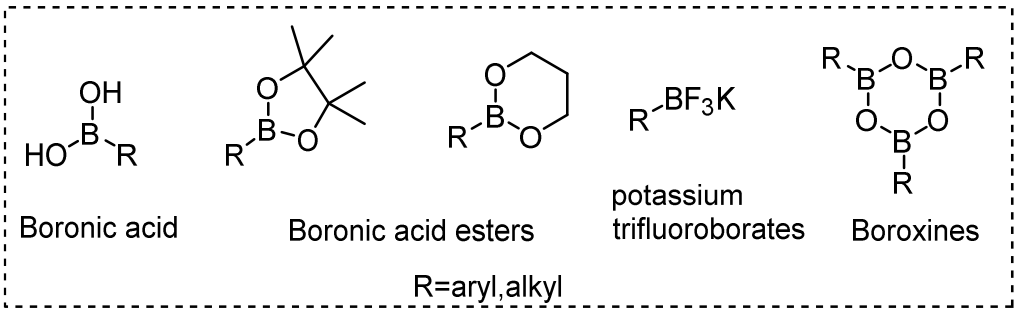

Figure **2.3** Boronic acid partners in Chan-Lam cross-coupling reaction

The nucleophiles

Amines are the predominant target nucleophiles in Chan–Lam cross-coupling reactions. Apart from aromatic amines other nitrogen heterocycles also undergo Chan-Lam cross-coupling. CEL couplings enable the formation of different types of Carbon–heteroatom bonds [45]. The target nucleophiles utilized in Chan–Lam cross-coupling strategy is shown in (Figure **2.4**). Other unique examples of CEL type C–O [46], C–P [47], C–Se [48], C-Te [49] and C–C [50] bond formations are also known, the scope of *N*-nucleophiles under Chan–Lam cross–coupling strategy is the most extensive one [51,52].

N-nucleophile:	Aryl and heteroaryl amines, aliphatic amines, Fused azaheterocycles, cyclic primary and secondary amines, lactams, carbamates, hydantoins
O-nucleophile	Phenols, urea, alcohols, water, carboxylic acids, hydroxylamine
S-nucleophile	Sulphonamides & *N*-arylsulfonamides, sulfoxines, arylthioureas, thiols, disulfides
Se/Te-nucleophile	Diselenides, Se, ditellurides
P-nucleophile	H-phosphonate diesters, H-phosphine oxides
C-nucleophile	Trifluoromethyltrimethylsilane, malonates, benzoic anhydrides

Figure **2.4** Nucleophiles utilized in Chan-Lam cross-coupling reaction

2.2.2 Mechanism for the Chan-Lam oxidative coupling reaction

Chan-Lam cross-coupling reaction is a net oxidative coupling of two nucleophiles; boronic acid and an amine. The key mechanistic steps involve coordination and transmetalation of the organoboron species to a Cu(II) center that is ligated to the nucleophiles (X). Disproportionation between CuX_2 complex and the Cu(II)-aryl(nucleophile) intermediate generates a Cu(III) species and an equivalent of Cu(I). Reductive elimination from the Cu(III) complex generates the coupled product and a second equivalent of Cu(I). In the final mechanistic step, the Cu(I) salts are oxidized back to Cu(II) *via* the terminal oxidant (Scheme **2.5**) [53,54].

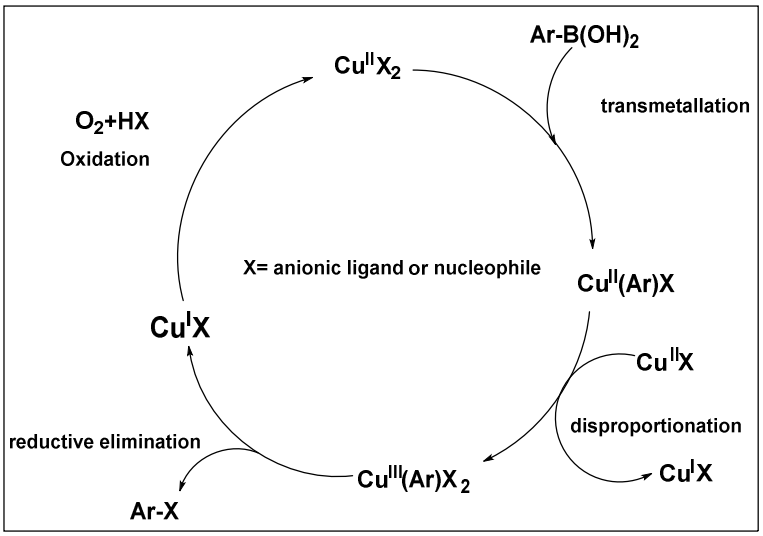

Scheme **2.5** Proposed mechanism of the Chan–Lam reaction

2.2.3 The Influence of ligands on the copper catalyst

Interestingly, the past decade witnessed a sharp increase on copper catalysed coupling reactions due to the important discovery on organic ligand facilitated copper catalysis, which significantly expanded the compatibility of copper catalysed couplings. The role of the ligand, although not clear, may be the stabilization of the Cu(l) species, increasing the solubility of catalyst in various solvents, milder temperatures (usually 80–100 °C) and helps to inhibit metal aggregation [55]. The ligands not only accelerated the reactions but also made them more reproducible and inherently safer [56]. The ligands used in Ullmann-type reactions were generally *N*-donors or mixed *N*– and *O*– donors, while *P*-based ligands were

generally found to be scarcely effective. Some of the successful ligands in copper mediated coupling reactions leading to arylations are shown (Figure **2.5**).

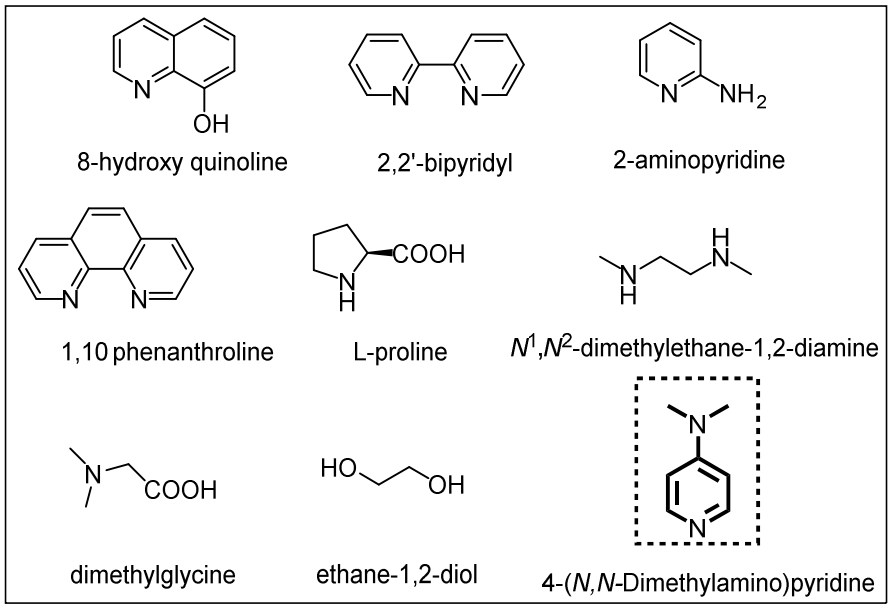

Figure **2.5** Ligands used in Cu- catalysed arylations

2.3 Background of the present work

Copper mediated arylation of *N*-nucleophiles (aromatic/heteroaromatic) with arylboronic acids for the construction of C–N bonds have been used as an efficient protocol for the formation of (hetero)aryl motifs. Although the Cu-catalyst promoted C–N cross-coupling would provide an efficient means in providing the valuable *N*-arylated heterocycles, the use of Chan–Lam type coupling in constructing heteroaromatic systems remains less explored. Here, we are focusing on some of the important representative reaction schemes of C–N bonds involving nitrogen containing heterocyclic moieties as nucleophiles.

In 1998, Lam and co-workers demonstrated *NH*-containing heteroaromatics such as imidazoles, triazoles, tetrazoles, pyrazoles, benzimidazoles, and indazoles as coupling partners. They used stoichiometric amount of $Cu(OAc)_2$ for the reaction. Azoles such as triazoles and tetrazoles, which are electron-poor, afforded the corresponding products in low yields, whereas pyrazoles and imidazoles gave good yields (Scheme **2.6**) [57].

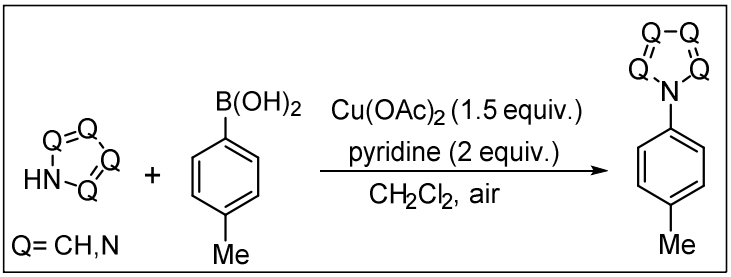

Scheme **2.6** $Cu(OAc)_2$ catalysed *N*-arylation of heteroaromatics

In 2001, the Collman group reported the synthesis of a wide range of *N*-arylimidazoles by the reaction of arylboronic acids and imidazoles using a novel copper complex $[Cu(OH)\cdot TMEDA]_2Cl_2$ (Scheme **2.7**). The optimal ratio of imidazoles and boronic acid in 2:1 molar ratio gives the product in a higher yield compared to a 1:1 molar ratio [58].

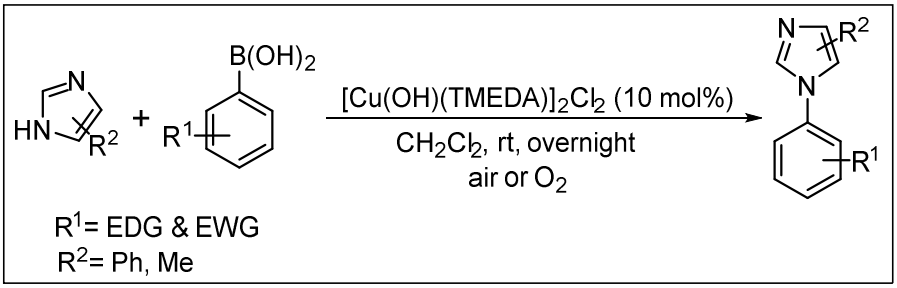

Scheme **2.7** $[Cu(OH)TMEDA]_2Cl_2$ catalysed *N*-arylation of imidazoles

In 2003, Lam and co-workers reported an efficient synthesis of C–N cross-coupling of a heterocyclic boronate with *NH*-containing heteroarenes. This constitutes the first successful copper promoted C–N cross-coupling involving a heterocyclic boronic acid system (Scheme **2.8**) [59].

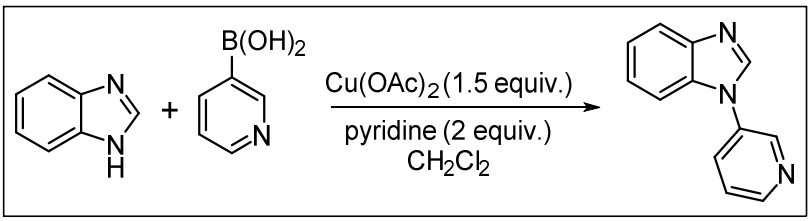

Scheme **2.8** $Cu(OAc)_2$ promoted C–N cross-coupling with pyridylboronates

In 2012, Han and co-workers reported the synthesis of 2,5-disubstituted tetrazoles *via* the direct coupling of N–H free tetrazoles and less toxic boronic acids in

presence of a catalytic amount of Cu_2O (5 mol%) as catalyst and 1 atm of environmentally benign O_2 as oxidant at 100 °C (Scheme **2.9**) [22].

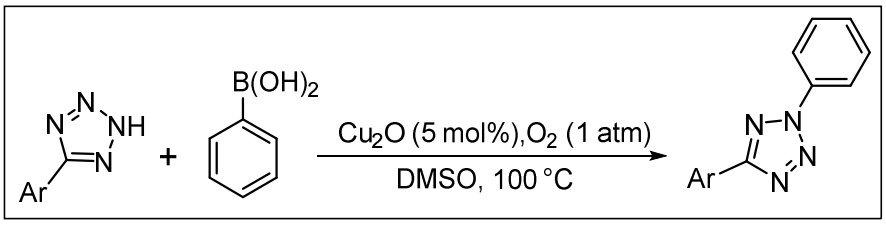

Scheme **2.9** Cu_2O catalysed N^2-arylation of tetrazoles

In 2014, Onaka and co-workers developed a mild and regioselective 2-arylation of 5-substituted tetrazoles with arylboronic acids using $[Cu(OH)(TMEDA)]_2Cl_2$ to generate 2,5-disubstituted tetrazoles (Scheme **2.10**). This is the first report of a highly regioselective arylation of 5-alkyltetrazoles [60].

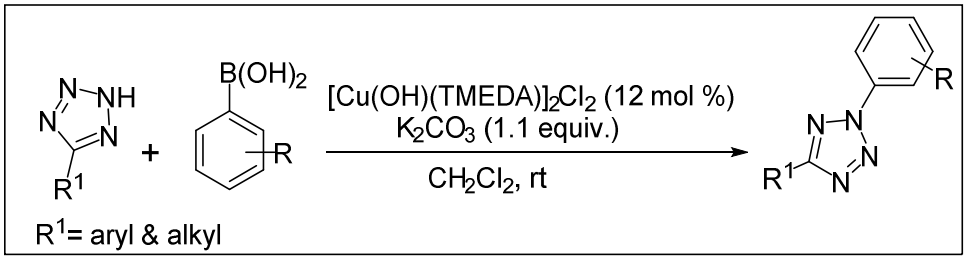

Scheme **2.10** $[Cu(OH)(TMEDA)]_2Cl_2$ catalysed N^2-arylation of tetrazoles with arylboronic acids

In 2016, Krasavin and Dar'in reported *N*-arylation of 2-imidazolines with arylboronic acids using $Cu(OAc)_2$ as catalyst in DMSO. Various 2-imidazolines and a number of boronic acids underwent smooth coupling to furnish *N*-aryl-2-imidazolines in moderate to good yields. The molar ratio of the substrate, boronic acid and $Cu(OAc)_2$ was taken in 1:2:1.5 and best yield was obtained with DMSO as solvent (Scheme **2.11**) [61].

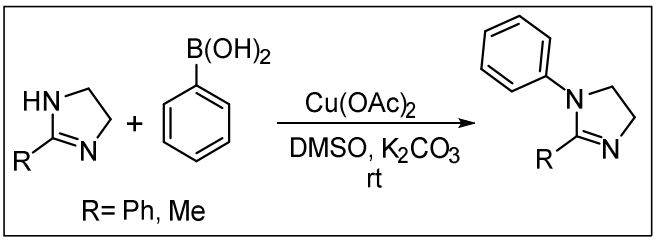

Scheme **2.11** $Cu(OAc)_2$ promoted *N*-Arylation of 2-imidazolines

In 2017, Tang and co-workers reported *N*-arylation of (benz)imidazoles with diarylboronic acid *via* $Cu(OAc)_2$ catalysed Chan-Lam cross-coupling assisted by tetramethylethylenediamine (TMEDA) in methanol in air at room temperature (Scheme **2.12**) [62].

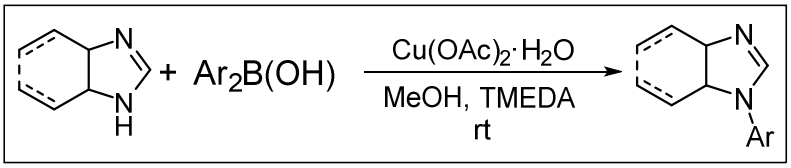

Scheme **2.12** $Cu(OAc)_2 \cdot 2H_2O$ catalysed *N*-arylation of (benz)imidazoles with diarylboronic acids

In 2017, Pale with co-workers developed a CuI-Zeolite catalyst (CuI-USY) which could be used in Chan-Lam cross-coupling reaction of arylboronic acids with a variety of *N*-nucleophiles. This catalytic system of easy recovery and recyclability could be reused to three times (Scheme **2.13**) [63].

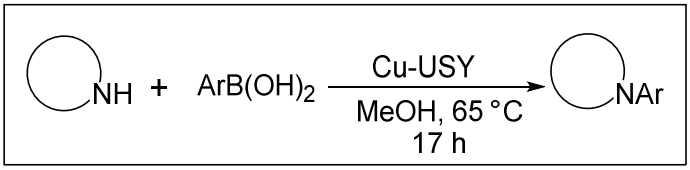

Scheme **2.13** CuI -USY catalysed Chan-Lam coupling reaction of arylboronic acids with a variety of *N*-nucleophiles

In 2018, Peng and group has carried out Chan–Lam coupling reactions of arylboronic acids with 1*H*-imidazole derivatives using *N,O*-bidentate ligand-tunable copper(II) complexes as a catalyst under base-free conditions (Scheme **2.14**) [41].

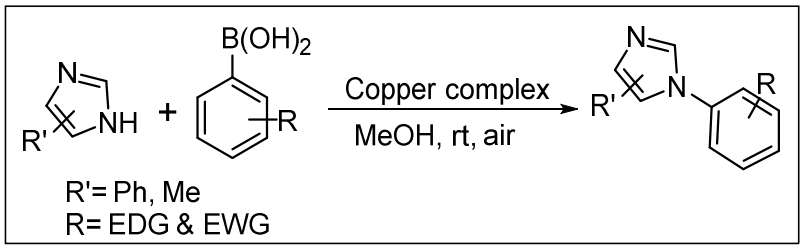

Scheme **2.14** *N*- arylation of 1*H*-imidazole derivatives using *N,O*-bidentate ligand-tunable copper(II) complexes as a catalyst

In 2019, Beletskaya and team has carried out copper-catalysed coupling of π-deficient N*H*-azoles with vinylboronic acids or vinyltrifluoroborate salt through 5

mol% of (phen)Cu(PPh_3)Br as a direct route to N^2-vinyl-1,2,3-triazoles and N^2-vinyltetrazoles (Scheme **2.15**) [20].

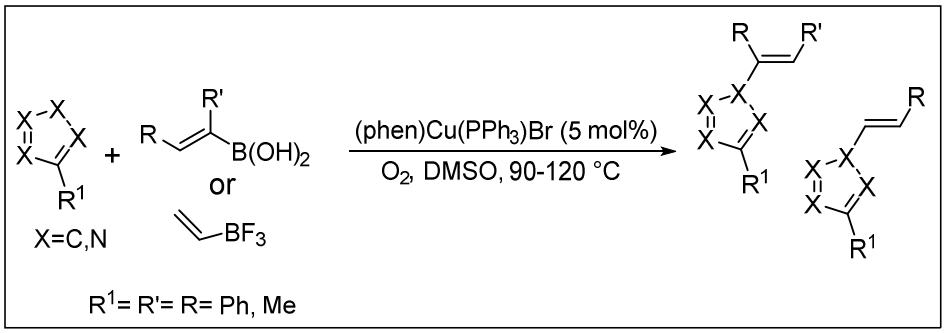

Scheme **2.15** Formation of N^2-vinyl-1,2,3-triazoles and N^2-vinyltetrazoles catalysed by (phen)Cu(PPh_3)Br

Very recently, Das and co-workers employed Chan-Lam amination for the arylation of hydantoins with substituted aryl/heteroaryl boronic acids assisted by CuF_2/MeOH under base and ligand-free conditions at room temperature and open air. The protocol produced various *N*-arylated hydantoins in excellent yields with exclusive regioselectivity (Scheme **2.16**) [19].

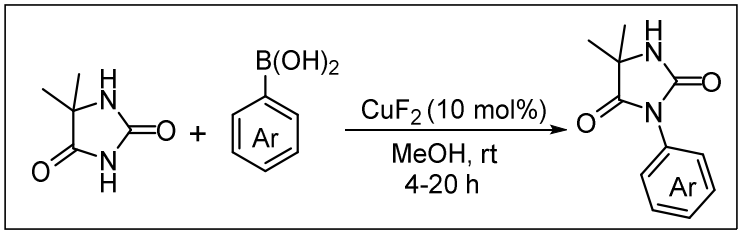

Scheme **2.16** *N*-arylation of hydantoin with substituted aryl heteroaryl boronic acids assisted by CuF_2/MeOH

2.4 Objectives of the present work

Recent studies have shown that there has been renewed interest in the preparation of tetrazoles as a substantial number of Active Pharmaceutical Ingredients (APIs) contains the tetrazole moiety in their structures. Also, reaction involving the formation of C–N bond is of utmost significance due to the occurrence of amine linkages in many molecules of biological importance. Interestingly, Chan-Lam methodology has appeared as an important synthetic tool for the development of such bonds. Despite the huge advances in the direct coupling of N*H*-free tetrazoles and boronic acid derivatives *via* copper catalysis, it still remains synthetically

challenging, owing to the regioselectivity issue. Also, the original Chan-Lam *N*-arylation procedure required excess amount of arylboronic acids, high-loading of copper salts and longer reaction time. It should be noted that the key to this envisioned protocol would be to control of regioselectivity as tetrazoles possess two nucleophilic sites and to improve the original procedure with respect to copper/ligand systems, solvents, bases and oxidative additives. We felt that this would be an excellent opportunity to present a facile and efficient protocol for the synthesis of regioselective 2,5-disubstituted tetrazoles by employing copper as the catalyst source. In this chapter, we envisioned developing a catalyst which is reliable, affordable, easy to prepare, provides regioselectivity and suitable for N^2-arylation of tetrazoles. The schematic representation of our protocol is shown below (Scheme **2.17**).

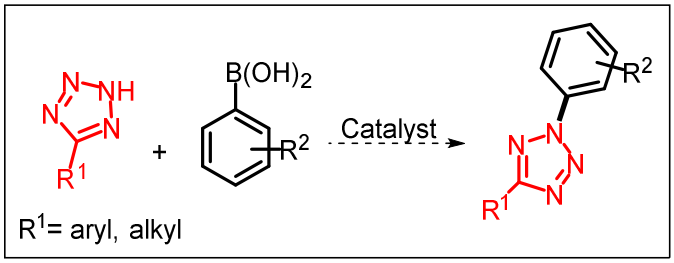

Scheme **2.17** Proposed scheme for N^2-arylation of tetrazoles

2.5 Results and Discussion

2.5.1 Synthesis of starting materials:

2.5.1.1 Synthesis of tetrazoles:

To validate the proposed scheme, we needed to synthesize a number of tetrazole substrates bearing different functional groups on aromatic ring of substituted phenyl tetrazoles. Several groups have reported different methods for the synthesis of tetrazoles. Among the reported synthetic routes to access tetrazoles, we synthesized 5-substituted-1*H*-tetrazoles from the one published by the Awasthi group without any alteration of the procedure, as already mentioned above (Scheme **2.2 1b**). 5-Methyl-1*H*-tetrazoles utilized for this work was procured commercially from Alfa Aesar. Synthesized tetrazoles are shown below (Scheme **2.18**).

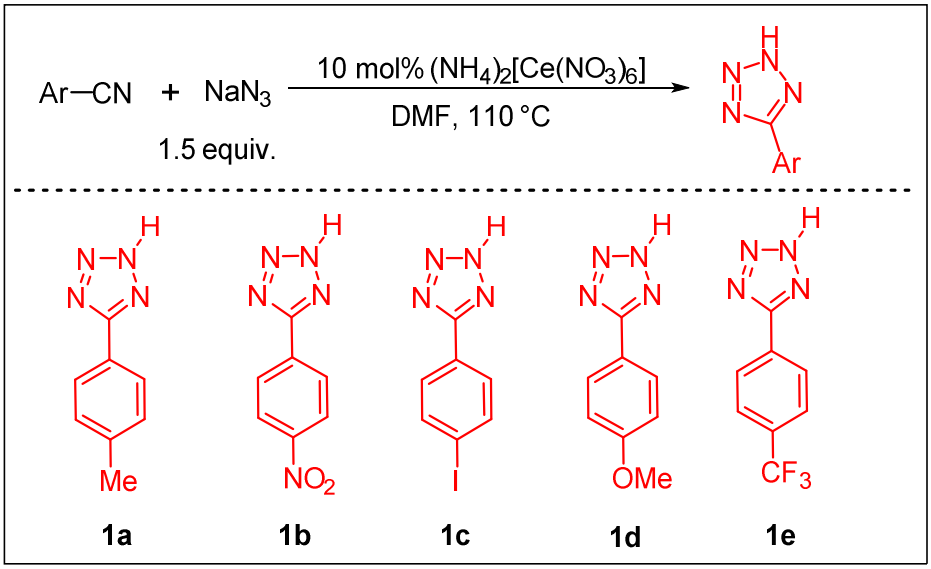

Scheme **2.18** Synthesized tetrazoles

2.5.1.2 Synthesis of the catalyst

At first, we began our experiment with the hope of finding an efficient copper catalytic system for N^2-arylation of tetrazoles using arylboronic acids. For that purpose, copper complex was prepared by stirring a mixture of $CuCl_2 \cdot 2H_2O$ and DMAP in 1:4 molar ratios in DMSO at room temperature for 3 hours. The mixture was further allowed to stand at room temperature. The pure crystals of the $[CuCl_2(DMAP)_4] \cdot 2.66H_2O$ complex were isolated in 87% yield after 2-3 days. The procedure is same as reported by Phukan [64] and his group with a change in the copper salt precursor.

2.5.2 Characterisation of the catalyst

It was first characterized by UV-Vis spectroscopy (a), powder X-ray diffraction analysis (p-XRD) (b) and then confirmed with single crystal XRD. The appearance of a strong peak at 644 nm in the UV-Vis spectrum and peaks at 2θ (19.05°, 20.78°, 28.52°) in the p-XRD indicate the existence of Cu(II) species (Figure **2.6**).

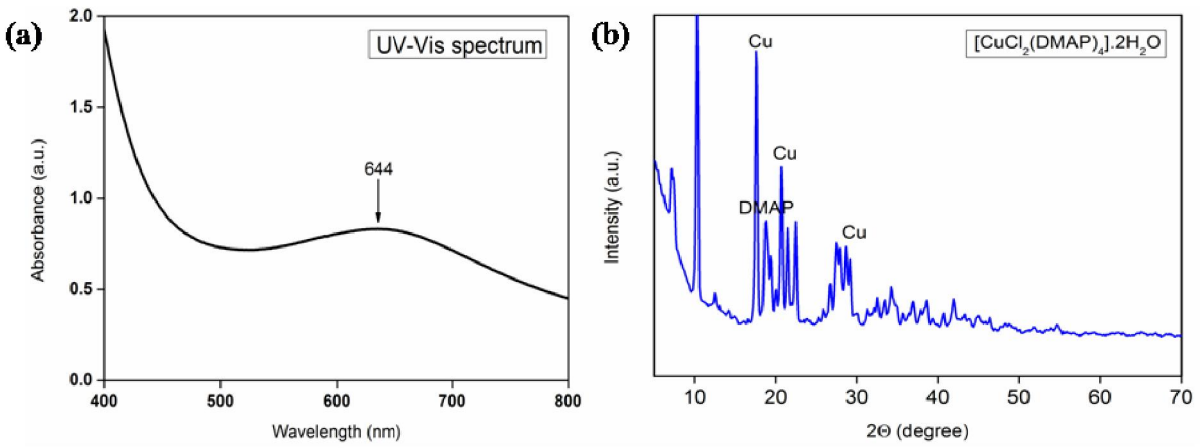

Figure **2.6** (a) UV-Vis spectrum of $[Cu(DMAP)_4Cl_2]\cdot 2.66H_2O$ and (b) p-XRD of the catalyst

Single crystal X-ray Diffraction (s-XRD) analysis

The single crystal structure of $[CuCl_2(DMAP)_4]\cdot 2.66H_2O$ was solved and refined in trigonal space group *R*-3, with half symmetry independent complex in the lattice (Figure **2.7**).

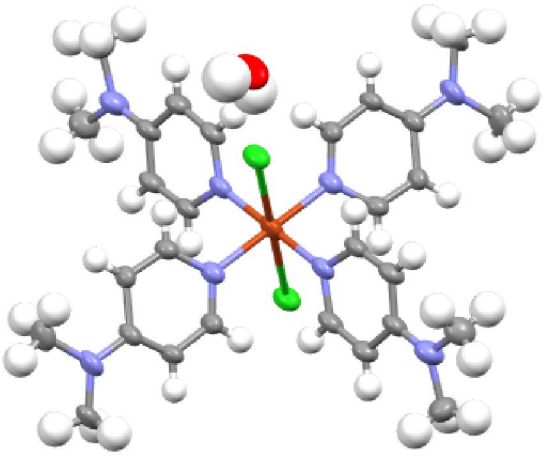

Figure **2.7** ORTEP of $[CuCl_2(DMAP)_4]\cdot 2.66H_2O$ with 50% probability ellipsoid. All the four *N*,*N*-Dimethyl pyridyl groups are positional disordered in two sites with equal probability of 50% and modelled. One half of the modelled molecule is shown for a clear view of the molecule, however a full ORTEP view with disordered modelled is available in the Appendix.

One water molecule is sitting in the special position with 33.33% occupancy leading to *R*-3 symmetry. All the four *N*,*N*-Dimethyl groups are positional disordered in two

sites with equal probability of 50% and modelled. The crystal data parameters are available in Table **2.1**.

Table 2.1 Crystallographic parameters of the catalyst complex $[CuCl_2(DMAP)_4]\cdot 2.66H_2O$

Crystal data	**$[CuCl_2(DMAP)_4]\cdot 2.66H_2O$**
Formula unit	$3(C_{28}H_{40}Cl_2CuN_8): 8(H_2O)$
Formula weight ($gmol^{-1}$)	2013.45
Crystal system	Trigonal
T [K]	100
a [Å]	24.673(3)
b [Å]	24.673(3)
c [Å]	14.092(3)
α [°]	90
β [°]	90
γ [°]	120
Volume [$Å^3$]	7429(2)
Space group	*R*-3
Z	3
D_{cal}[g/cm^3]	1.347
R_1, *w*R2	0.0413, 0.0782
Instrument	Bruker CCD Apex II
CCDC No	**2250662**

The lattice waters form an octamer sitting all 8 water molecules at the corner of a cube. These water cubes connect the complex along [001] axis through O–H···Cl strong hydrogen bonding. Experimental section is referred for the details of the Single crystal X-ray data collection methods and ORTEP (50% probability ellipsoid).

2.6 Optimization of the reaction conditions

We commenced our investigation of the cross-coupling reaction by taking 5-phenyltetrazole and phenylboronic acid as model substrates using the copper

ligand catalyst system for initial optimization of reaction conditions and the results are summarised in Table **2.2**.

At first, $CuCl_2 \cdot 2H_2O$ (5 mol%) and DMAP (5 mol%) (Table **2.2**, entry 1) were taken individually, and the desired product obtained was 53%. In the next step, increasing the $CuCl_2 \cdot 2H_2O$ loading to 10 mol% and DMAP to 10 mol% (Table **2.2**, entry 2), we observed an increase in product yield. Interestingly, upon varying mol% ratios of $CuCl_2 \cdot 2H_2O$ and DMAP, a significant increase in yield was observed (Table **2.2**, entries 3-5). With an intention to get better reaction yield, we have carried out an investigation to study the catalytic activity of the synthesized octahedral $[CuCl_2(DMAP)_4] \cdot 2.66H_2O$ complex. Accordingly, an experiment was carried out in presence of catalytic amount (10 mol%) of the octahedral complex, and it was found that yield of 2,5-disubstituted-1*H*-tetrazole **3a** (Table **2.2,** entry 6) significantly improved to 82% at 100 °C in 6 h. Upon increasing the catalyst loading to 20 mol%, no significant improvement in product yield was seen and notably upon decreasing the same to 5 mol%, product yield dropped to 59% (Table **2.2,** entries 7 and 8). Careful optimization of the reaction conditions unveiled that 10 mol% of the copper complex was sufficient for the reaction. Subsequently, other reaction parameters such as solvents, catalyst loadings, reaction temperature and time were examined with the model substrates. In presence of the catalyst, the best optimised results were obtained in 6 h compared to 12 h (Table **2.2**, entry 6). Among various solvents evaluated in the reaction, DMSO (Table **2.2**, entry 6) was found to be superior to DMF (Table **2.2**, entry 9) and no product formation was observed in presence of other solvents such as ACN, 1,4-dioxane and ethanol (Table **2.2**, entries 10-12). However, when the reaction temperature was lowered to 80 °C and 60 °C (Table **2.2**, entries 13 and 14) it led to a decrease in the product yield. With increase in reaction temperature to 120 °C, no significant improvement in yield was observed (Table **2.2**, entry 15). It was also observed that in absence of copper complex the reaction did not proceed (Table **2.2**, entry 16). Moreover, to investigate the role of DMAP, the reaction was carried out without it and the desired product **3a** was not obtained, which clearly indicates the essentiality of DMAP (Table **2.2**, entry 21). Interestingly, the use of pre-formed complex as a catalyst gave comparatively higher yield of the desired product than adding them

individually (Table **2.2**, entries 6 and 7). Also, we studied the reaction under open air flask where the results were consistent under O_2 atmosphere. Other copper salts such as $CuSO_4 \cdot 5H_2O$, $Cu(OAc)_2 \cdot H_2O$, $CuCl_2$ and CuI, gave poor results under the same reaction conditions (Table **2.2** entries 17-20). Furthermore, the regioselectivity of our reaction can be rationalised through the possible steric environment around the metal centre. Therefore, a combination of 10 mol% $[CuCl_2(DMAP)_4] \cdot 2.66H_2O$ complex, solvent DMSO and aerial oxygen were found to be crucial for the reaction to furnish the desired product, **3a** (Table 2.2, entry 6). This study helped us to deduce the optimised reaction conditions, which could be applied for the synthesis of the mentioned class of compounds.

Table 2.2 Optimization of reaction conditions[a]

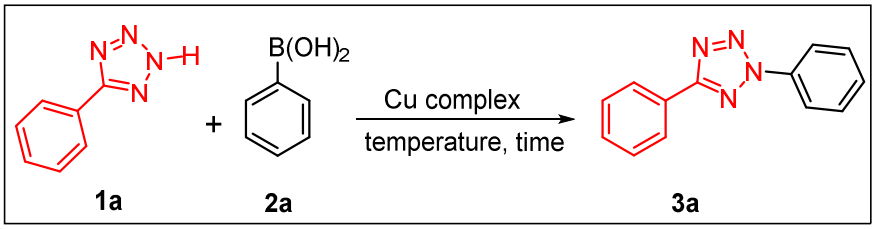

Entry	Catalyst (mol%)	Solvent (mL)	Temp. (°C)	Time (h)	Yield[b] (%) 3a
1	$CuCl_2 \cdot 2H_2O$ (5)/DMAP (5)	DMSO	100	12	53
2	$CuCl_2 \cdot 2H_2O$ (10)/DMAP (10)	DMSO	100	12	61
3	$CuCl_2 \cdot 2H_2O$ (10)/DMAP (20)	DMSO	100	12	69
4	$CuCl_2 \cdot 2H_2O$ (10)/DMAP (30)	DMSO	100	12	73
5	$CuCl_2 \cdot 2H_2O$ (10)/DMAP (40)	DMSO	100	12	77
6	**$[CuCl_2(DMAP)_4] \cdot 2.66H_2O$ (10)**	**DMSO**	**100**	**6**	**82**
7	$[CuCl_2(DMAP)_4] \cdot 2.66H_2O$ (20)	DMSO	100	6	83
8	$[CuCl_2(DMAP)_4] \cdot 2.66H_2O$ (5)	DMSO	100	6	59
9	$[CuCl_2(DMAP)_4] \cdot 2.66H_2O$ (10)	DMF	100	6	39
10	$[CuCl_2(DMAP)_4] \cdot 2.66H_2O$ (10)	ACN	100	6	nr
11	$[CuCl_2(DMAP)_4] \cdot 2.66H_2O$ (10)	1,4-dioxane	100	6	nr
12	$[CuCl_2(DMAP)_4] \cdot 2.66H_2O$ (10)	ethanol	80	6	nr
13	$[CuCl_2(DMAP)_4] \cdot 2.66H_2O$ (10)	DMSO	60	6	trace
14	$[CuCl_2(DMAP)_4] \cdot 2.66H_2O$ (10)	DMSO	80	6	46

15	$[CuCl_2(DMAP)_4]\cdot 2.66H_2O$ (10)	DMSO	120	6	76
16	-	DMSO	100	6	nr
17	$Cu(OAc)_2\cdot H_2O$ (10)/DMAP (10)	DMSO	100	6	nr
18	$CuSO_4\cdot 5H_2O$ (10)/DMAP (10)	DMSO	100	6	nr
19	CuCl (10)/DMAP (10)	DMSO	100	6	53
20	CuI (10)/DMAP (10)	DMSO	100	6	57
21	$CuCl_2\cdot 2H_2O$(10)	DMSO	100	6	nr

[a]Reaction Conditions: ***1a*** *(0.5 mmol),* ***2a*** *(0.65 mmol), solvent (3 mL).* [b]*Yields are obtained from the* ^{1}*H NMR spectra; nr = no reaction*

2.6.1 Substrate scope study

Having established the optimized reaction conditions, we set to utilize the methodology to determine the scope of phenylboronic acids and tetrazoles bearing electron-donating groups (EDG), electron-withdrawing groups (EWG) as well as sterically hindered ones.

Initially, the effect of substituents on the benzene ring of phenylboronic acid was examined. The coupling of 5-aryltetrazoles with phenylboronic acid was allowed in the presence of $[CuCl_2(DMAP)_4]\cdot 2.66H_2O$ catalyst and the reaction proceeded well, giving the corresponding 2,5-disubstituted product in 82% yield (Table **2.3**, entry 3a). It is to be noted that, the phenyl group was introduced at N^2-position in these reactions. The reaction of **1a** with various derivatives of **2a**, (and *vice-versa*) proceeded efficiently furnishing the corresponding 2*H*-arylated tetrazoles in moderate to good yields. We observed that phenyl tetrazoles reacted efficiently with substituted phenylboronic acids having EDGs such as -Me, -OMe, $-C(CH_3)_3$ (Table **2.3**, entries 3b-3f) at *para* position. Decrease in yield was observed with EWG i.e. -Cl substituent in the boronic acid ring (Table **2.3**, entry 3g). In comparison to EWGs on the boronic acid, EDGs provided better yields of the N^2-arylated product.

Table **2.3 Substrate scope study** [a]

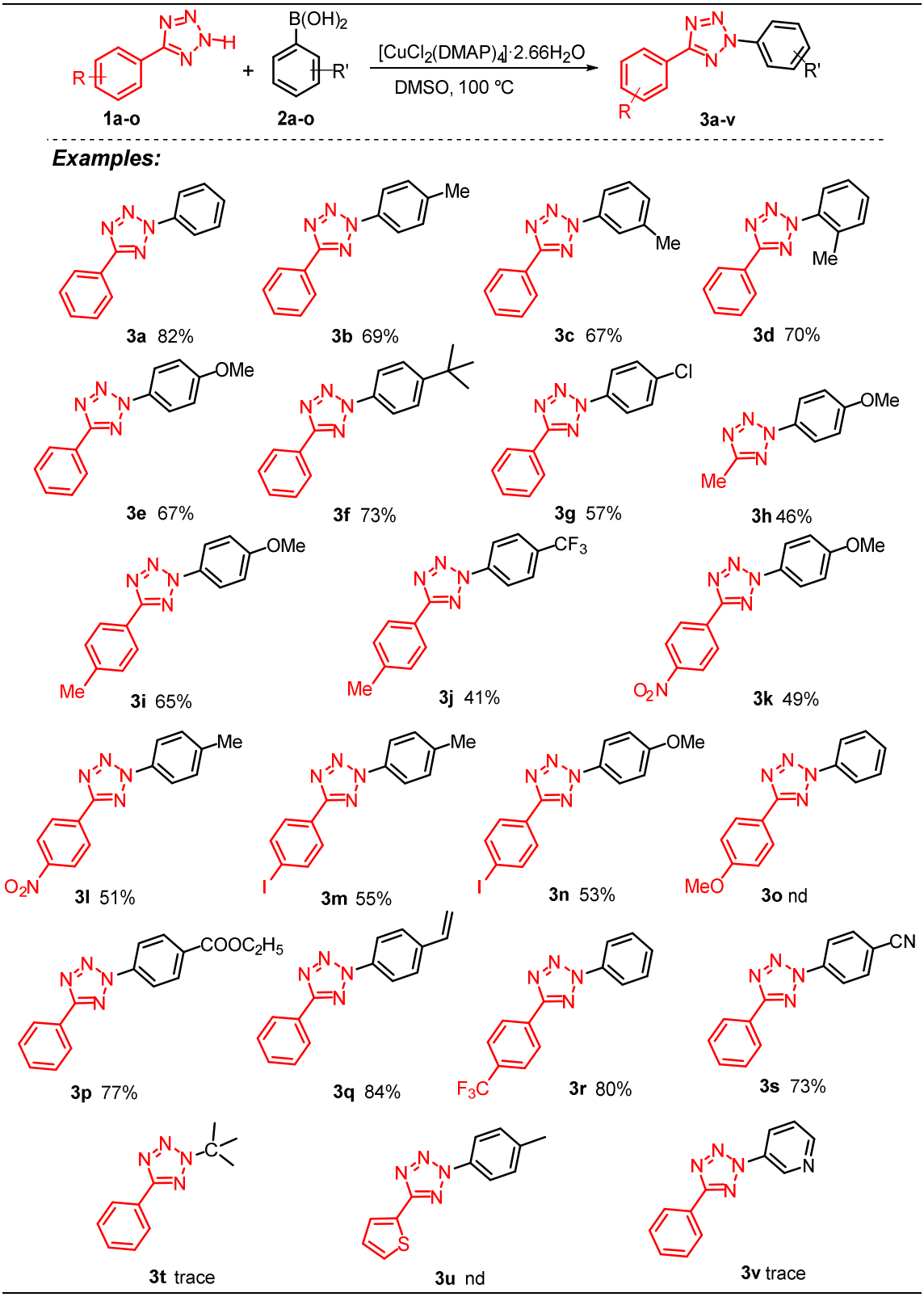

[a]*Reaction conditions: 1 (0.5 mmol), 2 (0.65 mmol), catalyst (10 mol%), solvent (3 mL) in a round-bottomed flask, nd: not detected .Yields are isolated yields.*

Under the optimized reaction condition, -I, -Me, -NO_2 substituted 5-phenyltetrazoles underwent smooth coupling with a range of phenylboronic acids. 2-(4-methylphenyl)-2*H*-tetrazole yield 65% yield with electron donating 4-methoxy phenylboronic acid (Table **2.3**, entry 3i) and decrease in yield was observed with phenylboronic acid having EWGs (Table **2.3,** entry 3j). Another phenyl tetrazole bearing a strong electron-withdrawing $-NO_2$ group in the phenyl ring periphery was also a competent substrate affording the corresponding regioisomers in good to moderate yields (Table **2.3**, entries 3k, and 3l). On the other hand, tetrazoles with an electron withdrawing group in the phenyl ring produced lesser yield as compared to tetrazoles bearing an electron pumping group which can be attributed to decrease in nucleophilicity in the tetrazole moiety by EWGs. Subsequently, iodo substituted phenyl tetrazoles were also tested, where good to moderate result was obtained with substituted phenylboronic acids (Table **2.3**, entries 3m, and 3n). Methoxy substituted phenyl tetrazoles failed to furnish the desired result (Table **2.3**, entry 3o). Another notable feature is that our catalyst system showed good regioselectivity, inertness towards reactive functionalities on the phenylboronic acid such as -Cl (Table **2.3**, entry 3g) which served as good nucleophiles or leaving groups in Cu-catalysed coupling reactions with phenylboronic acids.

A key challenge in TM-catalysed C–N bond formation in tetrazoles is controlling the regio- and chemo-selectivity. In this reaction, our catalyst has emerged as a promising mode to achieve selective N^2-arylation. Thus, our protocol was found to be applicable for a wide range of electronically diverse phenylboronic acids and phenyl tetrazoles with good yields of the isolated product. It was also seen that pyridine boronic acid and alkyl boronic acid (Table **2.3,** entries 3t and 3v) yielded trace amount whereas arylation of 5-(thiophen-2-yl)-2*H*-tetrazole was not detected (Table **2.3,** entry 3u) with our optimized protocol.

It is to be noted that Chan-Lam reactions usually require boronic acids in excess, which promote undesirable side pathways such as homo coupling product, phenol derived from the phenyl boronic acids. But in our reaction, very less amount of homo coupled by-products were noticed.

2.7 Controlled experiment

A controlled experiment was carried out to confirm the crucial role of O_2 as an ancillary oxidant and $[CuCl_2(DMAP)_4]\cdot 2.66H_2O$ as catalyst in this transformation. When the reaction was carried out in presence of other organic bases such as NEt_3, DBU and DABCO; although the formation of *N*-arylated product was observed; the conversion rate was very low. This result clarified the efficiency of DMAP in our reaction condition. To our notice, DMAP's role both as ligand and base helped our system to avoid use of any additional base in the reaction. Moreover, no product formation was observed in presence of N_2 atmosphere that determines the essentiality of oxygen in the reaction (Scheme **2.19**).

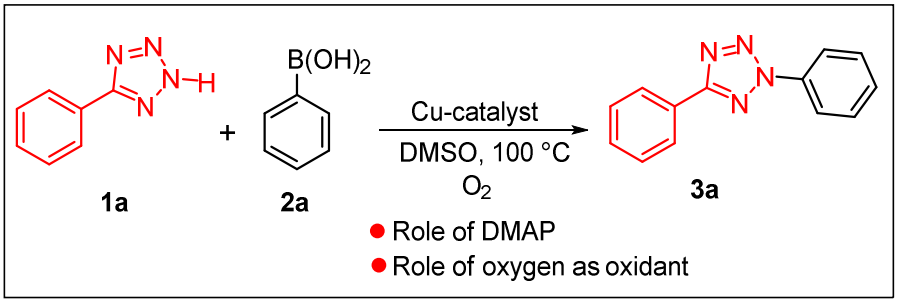

Scheme **2.19** N^2-arylation of tetrazoles with phenylboronic acid

The single crystal XRD study showed that the catalyst $[CuCl_2(DMAP)_4]\cdot 2.66H_2O$ was octahedral in shape with two chlorine atoms situated 2.81 Å away from the central copper atom compared to a general Cu–Cl bond which is 2.2 Å. Hence, displacement of the loosely bound chlorine atoms was much easier to form the intermediate transmetalated species. This could be the reason for enhancement of the reaction rate of the C–N bond formation between tetrazole and phenylboronic acid derivatives. From the literature reports, the best plausible mechanism available for the formation of C–N bond was proposed by Chan-Lam. We believed that the mechanism of the developed reaction falls under the ambit of Chan-Lam cross-coupling mechanism. A plausible mechanism has been proposed here for this reaction, but detailed mechanistic study of the reaction has not been condcuted, but it is certainly under the scope of ongoing studies.

A plausible mechanism could be proposed considering the $[CuCl_2(DMAP)_4]\cdot 2.66H_2O$ catalyst. In the initial step displacement of DMAP and

two chlorine atoms from the octahedral complex followed by formation of Tz–copper(II) intermediate (**A**). The intermediate (**A**) then undergoes transmetalation with phenylboronic acid to form complex (**B**). Disproportionation of copper(II) complex (**C**) gives rise to copper(III) intermediate followed by reductive elimination to N^2-arylated product (**D**) with simultaneous formation of a copper(I) species. Finally, terminal oxidation of copper(I) species (**E**) to copper(II) by molecular oxygen completes the catalytic cycle [65].

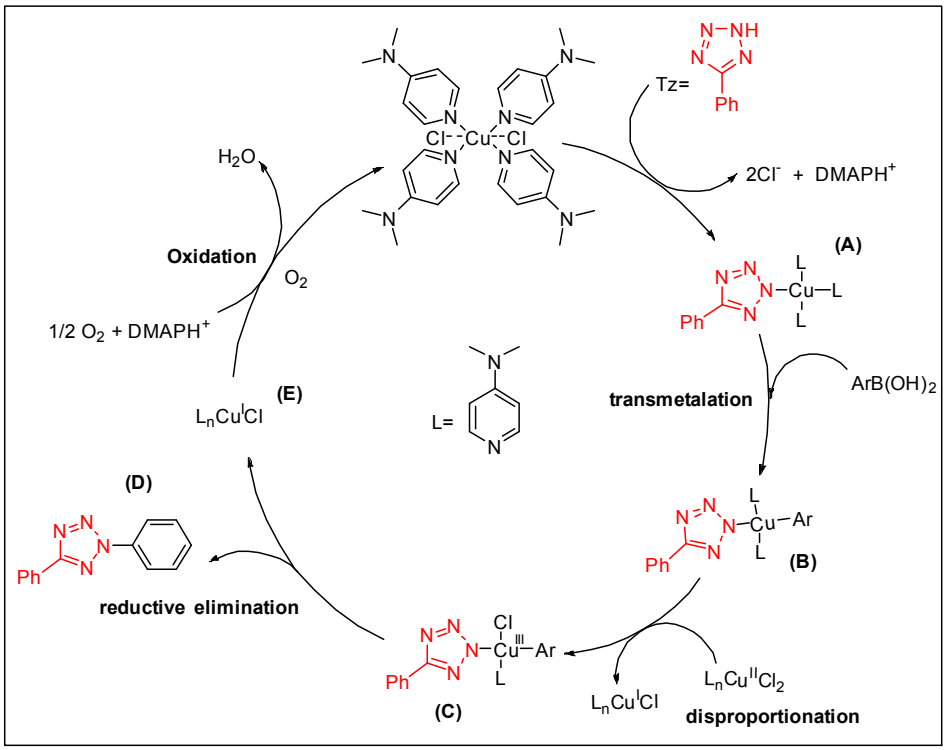

Scheme **2.20** Plausible mechanism for C–N bond formation

2.8 Conclusion

In conclusion, it can be stated that we have developed a $[CuCl_2(DMAP)_4]\cdot 2.66H_2O$ catalytic system for the regioselective synthesis of 2,5-disubstituted-1*H*-tetrazoles. The developed catalyst is cheap, easy to prepare, provides regioselectivity and suitable for N^2-arylation. It exhibits general reactivities to both arylated and alkylated tetrazoles. The products are purely regio-isomers obtained in considerably good yields. The protocol successfully offers a facile and practical way to deliver regio-selective 2,5-disubstituted tetrazoles.

2.8.1 Experimental Section

2.8. 1.1 General procedure for the arylation of tetrazoles

$[Cu(DMAP)_4Cl_2]\cdot 2.66H_2O$ complex (10 mol%) was added to a mixture of phenyl tetrazole (0.5 mmol) and phenyl boronic acid (0.65 mmol) in DMSO (3 mL) and the mixture was stirred at 100 °C for 6 hours. The progress of the reaction was monitored by TLC. On completion of the reaction, the crude mixture was extracted using ethyl acetate (10 mL) and washed with ice water (20 mL). The organic layer was further concentrated under reduced pressure to obtain the crude product. The crude product was purified by column chromatography on silica gel (hexane–EtOAc, 95:5) to afford the *N*–arylated tetrazoles (**3a-s**).

2.8.1.2 Characterisation data of the products

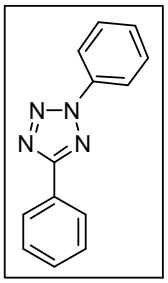

2,5-diphenyl-2H-tetrazole (**3a**)

Yellow solid (91.05 mg, 82%); IR (neat, cm^{-1}) 3073, 2928, 2842, 1957, 1820, 1590, 1482, 1338, 1202, 993, 892; ^1H NMR (400 MHz, $CDCl_3$) δ (ppm) 8.18 (dd, J = 7.7, 1.9 Hz, 2H), 8.22–8.15 (m, 2H), 7.54–7.37 (m, 6H); ^{13}C NMR (100 MHz, $CDCl_3$) δ (ppm) 165.5, 136.9, 130.6, 129.7, 129.6, 129.0, 127.2, 127.1, 119.9.

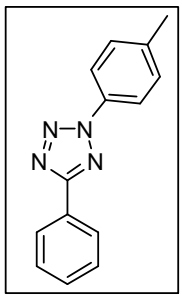

5-phenyl-2-(p-tolyl)-2H-tetrazole (**3b**)

Light yellow solid (81.45 mg, 69%); IR (neat, cm^{-1}) 3044, 2928, 2842, 1965, 1799, 1583, 1489, 1367, 1208, 1079, 993, 892; ^1H NMR (400 MHz, $CDCl_3$) δ (ppm) 8.16 (d, J = 9.4 Hz, 2H), 7.97 (d, J = 8.5 Hz, 2H), 7.42 (d, J = 7.3 Hz, 3H), 7.26 (d, J = 8.3 Hz, 2H), 2.35 (s, 3H); ^{13}C NMR (100 MHz, $CDCl_3$) δ (ppm) 165.1, 139.9, 134.7, 130.5, 130.2, 128.9, 127.3, 127.0, 119.7, 21.2.

5-phenyl-2-(m-tolyl)-2H-tetrazole (**3c**)

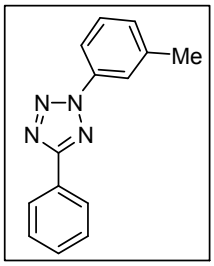

Pink solid (79.09 mg, 67%); IR (neat, cm^{-1}); 3080, 2922, 2849, 2346, 1972, 1876, 1604, 1467, 1208, 1086, 1014; ^1H NMR (400 MHz, $CDCl_3$) δ (ppm) 8.17 (d, J = 8.0 Hz, 2H), 7.90 (d, J = 8.2 Hz, 2H), 7.43 (d, J = 7.2 Hz, 3H), 7.34 (d, J = 7.9 Hz, 1H), 7.21 (d, J = 7.7 Hz, 1H), 2.39 (s, 3H); ^{13}C NMR (100 MHz, $CDCl_3$) δ (ppm) 165.2, 139.4, 136.9, 130.5, 130.4, 129.5, 128.9, 126.9, 120.4, 117.0, 21.6. HRMS (ESI-TOF) m/z $(M+H)^+$ calculated for $C_{14}H_{13}N_4^+$, 237.1135 found, 237.1135

5-phenyl-2-(o-tolyl)-2H-tetrazole (**3d**)

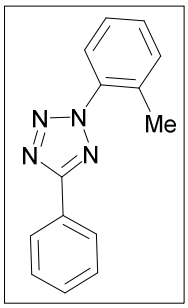

White solid (82.63 mg, 70%); IR (neat, cm^{-1}) 3073, 2932, 2840, 2300, 1965, 1881, 1594, 1389, 1222, 1178, 1110, 1012; ^1H NMR (500 MHz, $CDCl_3$) δ (ppm) 8.25 (dd, J = 7.5, 2.1 Hz, 2H), 7.66 (d, J = 7.7 Hz, 1H), 7.51 (d, J = 7.6 Hz, 3H), 7.47 – 7.32 (m, 3H), 2.43 (s, 3H); ^{13}C NMR (125 MHz, $CDCl_3$) δ (ppm) 165.0, 136.5, 133.1, 131.9, 130.5, 130.3, 129.0, 127.3, 127.0, 126.9, 125.3, 18.8.

2-(4-methoxyphenyl)-5-phenyl-2H-tetrazole (**3e**)

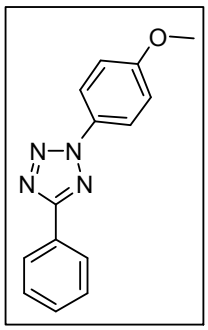

Yellow solid (84.45 mg, 67%); IR (neat, cm^{-1}) 3073, 2922, 2857, 1899, 1597, 1511, 1461, 1208, 1072, 986, 806; ^1H NMR (400 MHz, $CDCl_3$) δ (ppm) 8.14 (d, J = 8.0 Hz, 2H), 7.99 (d, J = 9.1 Hz, 2H), 7.41 (d, J = 7.5 Hz, 3H), 6.94 (d, J = 9.1 Hz, 2H), 3.77 (s, 3H); ^{13}C NMR (100 MHz, $CDCl_3$) δ (ppm) 164.6, 160.8, 130.8, 128.9, 127.3, 126.6, 121.4, 114.7, 55.4.

2-(4-(tert-butyl)phenyl)-5-phenyl-2H-tetrazole (**3f**)

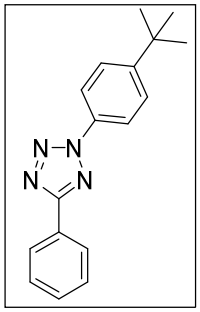

Brown liquid (101.81 mg, 73%); IR (neat, cm^{-1}) 3073, 2950, 2864, 2338, 1511, 1439, 1353, 1251, 1208, 1108, 993; ^1H NMR (400 MHz, $CDCl_3$) δ (ppm) 8.18 (d, J = 9.5 Hz, 2H), 8.02 (d, J = 8.8 Hz, 2H), 7.50 (d, J = 8.8 Hz, 2H), 7.44 (d, J = 7.4 Hz, 3H), 1.30 (s, 9H); ^{13}C NMR (100 MHz, $CDCl_3$) δ (ppm) 165.2, 153.2, 134.4,

130.4, 128.9, 127.3, 127.0, 126.5, 119.2, 31.0. HRMS (ESI-TOF) m/z $(M+H)^+$ calculated for $C_{17}H_{19}N_4^+$, 279.1604 found, 279.1610.

2-(4-chlorophenyl)-5-phenyl-2H-tetrazole (**3g**)

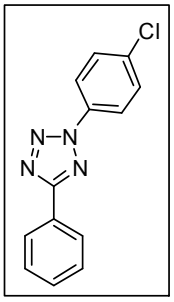

Yellow solid (72.97 mg, 57%); IR (neat, cm^{-1}) 3094, 2928, 2842, 1892, 1525, 1489, 1461, 1403, 1274, 1079, 1000, 813,784; ^1H NMR (400 MHz, $CDCl_3$) δ (ppm) 8.06 (d, J = 8.9 Hz, 2H), 8.15 (d, J = 7.9 Hz, 2H), 7.48 – 7.40 (m, 5H). ^{13}C NMR (100 MHz, $CDCl_3$) δ (ppm) 165.5, 135.5, 135.4, 130.7, 129.9, 129.0, 127.0, 126.9, 121.0.

2-(4-methoxyphenyl)-5-methyl-2H-tetrazole (**3h**)

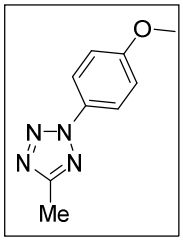

Brown liquid (43.72 mg, 46%); IR (neat, cm^{-1}) 2950, 2915, 2849, 1878, 1604, 1518, 1432, 1367, 1245, 1172, 1093, 1022, 827; ^1H NMR (400 MHz, $CDCl_3$) δ (ppm) 8.01 – 7.85 (m, 2H), 7.05 – 6.89 (m, 2H), 3.81 (s, 3H), 2.55 (s, 3H). ^{13}C NMR (100 MHz, $CDCl_3$) δ (ppm) 160.4, 160.4, 130.4, 121.5, 114.3, 55.8, 11.0.

2-(4-methoxyphenyl)-5-(p-tolyl)-2H-tetrazole (**3i**)

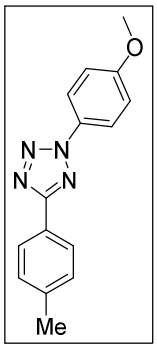

Yellow solid (86.48 mg, 65%); IR (neat, cm^{-1}) 3080, 2950, 2842, 1899, 1726, 1612, 1504, 1439, 1266, 1165, 1014, 827; ^1H NMR (400 MHz, $CDCl_3$) δ (ppm) 8.01 (dd, J = 14.8, 8.6 Hz, 4H), 7.22 (d, J = 8.0 Hz, 2H), 6.94 (d, J = 9.1 Hz, 2H), 3.78 (s, 3H), 2.33 (s, 3H). ^{13}C NMR (100 MHz, $CDCl_3$) δ (ppm) 165.1, 160.4, 140.6, 130.5, 129.6, 126.9, 124.5, 121.4, 114.6, 55.6.

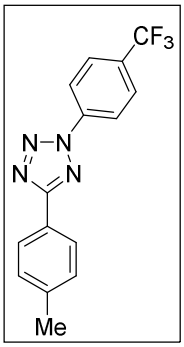

5-(p-tolyl)-2-(4-(trifluoromethyl)phenyl)-2H-tetrazole (**3j**)

White solid (62.33 mg, 41%); IR (neat, cm^{-1}) 3108, 2915, 2849, 1907, 1604, 1511, 1432, 1338, 1266, 1108, 1000, 856; ^1H NMR (400 MHz, $CDCl_3$) δ (ppm) 8.11 (d, J = 9.0 Hz, 2H), 8.05 (d, J = 8.0 Hz, 2H), 7.26 (d, J = 8.0 Hz, 2H), 7.18 (d, J = 7.4 Hz, 2H), 2.36 (s, 3H); ^{13}C NMR (100 MHz, $CDCl_3$) δ (ppm) 165.4, 140.9, 129.7, 127.0, 124.2, 121.9, 121.8, 116.8, 116.6, 21.6. HRMS (ESI-TOF) m/z $(M+H)^+$ calculated for $C_{15}H_{12}F_3N_4^+$, 305.1009 found, 305.1009

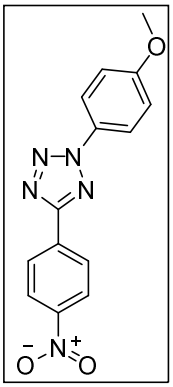

2-(4-methoxyphenyl)-5-(4-nitrophenyl)-2H-tetrazole (**3k**)

White solid (72.83 mg, 49%); IR (neat, cm^{-1}) 2922, 2857, 1892, 1597, 1504, 1331, 1251, 1208, 1108, 1022, 820; ^1H NMR (400 MHz, $CDCl_3$) δ (ppm) 8.34 (dd, J = 21.9, 8.0 Hz, 2H), 7.90 (d, J = 8.4 Hz, 1H), 8.04 (dd, J = 11.4, 9.1 Hz, 2H), 7.79 (d, J = 8.4 Hz, 1H), 6.99 (d, J = 9.3 Hz, 2H), 3.84 (s, 3H); ^{13}C NMR (100 MHz, $CDCl_3$) δ (ppm) 160.7, 148.8, 138.4, 128.5, 128.2, 126.6, 123.7, 121.1, 114.4, 56.4

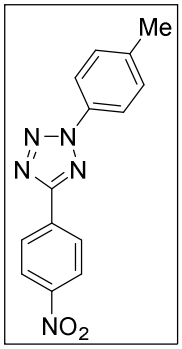

5-(4-nitrophenyl)-2-(p-tolyl)-2H-tetrazole (**3l**)

Dirty White solid (71.67 mg, 51%); IR (neat, cm^{-1}) 3073, 2915, 2857, 1914, 1604, 1525, 1360, 1093, 1000, 849, 727; ^1H NMR (400 MHz, $CDCl_3$) δ (ppm) 8.35 (d, J = 8.8 Hz, 2H), 8.30 (d, J = 8.8 Hz, 2H), 7.99 (d, J = 8.4 Hz, 2H), 7.31 (d, J = 8.4 Hz, 2H), 2.39 (s, 3H); ^{13}C NMR (100 MHz, $CDCl_3$) δ (ppm)163.4, 149.0, 140.3, 134.4, 132.9, 130.3, 127.9, 124.5, 119.8, 20.9.

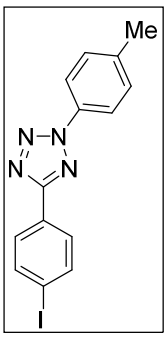

5-(4-iodophenyl)-2-(p-tolyl)-2H-tetrazole (**3m**)

White solid (99.55 mg, 55%); IR (neat, cm^{-1}) 3094, 2994, 2828, 1604, 1504, 1439, 1259, 1180, 993, 834; ^1H NMR (400 MHz, $CDCl_3$) δ (ppm) 7.95 (d, J = 8.5 Hz, 2H), 7.88 (d, J = 8.4 Hz, 2H), 7.77 (d, J = 8.4 Hz, 2H), 7.27 (d, J = 8.4 Hz, 2H), 2.36 (s, 3H); ^{13}C NMR (100 MHz, $CDCl_3$) δ (ppm) 164.2, 140.1, 138.4, 134.3, 130.1, 128.8, 126.6, 120.1, 96.9, 21.4. HRMS (ESI-TOF) m/z $(M+H)^+$ calculated for $C_{14}H_{12}IN_4^+$, 363.0101 found, 363.0101

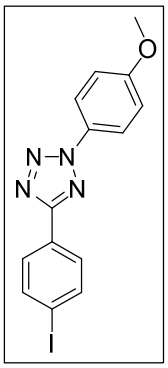

5-(4-iodophenyl)-2-(4-methoxyphenyl)-2H-tetrazole (**3n**)

White solid (100.17 mg, 53%); IR (neat, cm^{-1}) 3065, 2928, 1892, 1583, 1461, 1251, 1195, 1022, 993, 820; ^1H NMR (400 MHz, $CDCl_3$) δ (ppm) 7.98 (d, J = 9.2 Hz, 2H), 7.86 (d, J = 8.3 Hz, 2H), 7.76 (d, J = 8.4 Hz, 2H), 6.95 (d, J = 9.1 Hz, 2H), 3.79 (s, 3H); ^{13}C NMR (100 MHz, $CDCl_3$) δ (ppm) 164.3, 160.4, 138.5, 130.4, 128.5, 126.9, 121.4, 114.7, 96.9, 55.4. HRMS (ESI-TOF) m/z $(M+H)^+$ calculated for $C_{14}H_{12}IN_4O^+$, 379.0050 found, 379.0016.

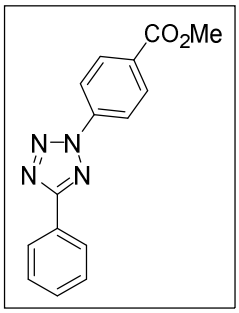

Methyl 4-(5-phenyl-2H-tetrazol-2-yl)benzoate (**3o**)

Off white solid (113.3 mg, 77%); IR (neat, cm^{-1}) 2988, 1765, 1654, 1445, 1339, 1105, 1057, 954, 765; ^1H NMR (400 MHz, $CDCl_3$) δ (ppm) 8.36 – 8.20 (m, 6H), 7.54 (dd, J = 5.6, 1.8 Hz, 3H), 3.98 (s, 3H). ^{13}C NMR (100 MHz, $CDCl_3$) δ (ppm) 165.8, 165.5, 139.7, 131.3, 131.1, 130.8, 129.0, 127.1, 126.8, 119.5, 52.5.

5-phenyl-2-(4-vinylphenyl)-2H-tetrazole (**3p**)

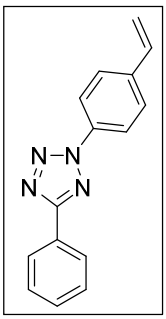

White solid (104.28 mg, 84%); IR (neat, cm^{-1}) 2978, 1624, 1504, 1473, 1397, 1258, 1063, 1019, 843; ^{1}H NMR (400 MHz, $CDCl_3$) δ (ppm) 8.32 – 8.20 (m, 2H), 8.19 – 8.06 (m, 2H), 7.64 – 7.41 (m, 5H), 6.77 (dd, J = 17.6, 10.9 Hz, 1H), 5.85 (d, J = 17.6 Hz, 1H), 5.37 (d, J = 10.9 Hz, 1H). ^{13}C NMR (100 MHz, $CDCl_3$) δ (ppm) 165.1, 138.9, 136.0, 135.4, 130.5, 128.9, 127.3, 127.18, 127.0, 119.9, 115.8. HRMS (ESI-TOF) m/z $(M+H)^+$ calculated for $C_{15}H_{13}N_4^+$, 249.1135 found, 249.1141

2-phenyl-5-(4-(trifluoromethyl)phenyl)-2H-tetrazole (**3q**)

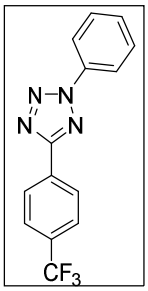

White solid flakes (116.1 mg, 80%); IR (neat, cm^{-1}) 2940, 1945, 1743, 1580, 1485, 1309, 1108, 900, 755; ^{1}H NMR (400 MHz, $CDCl_3$) δ (ppm) 8.56 – 8.39 (m, 2H), 8.20 (ddd, J = 8.4, 4.1, 2.4 Hz, 2H), 7.79 – 7.45 (m, 5H). ^{13}C NMR (100 MHz, $CDCl_3$) δ (ppm) 164.0, 136.7, 130.1, 129.9, 129.7, 129.7, 129.5, 124.7, 119.8.

4-(5-phenyl-2H-tetrazol-2-yl)benzonitrile (**3r**)

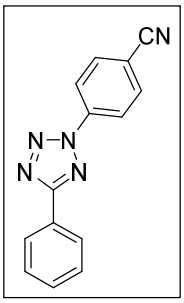

off white solid (90.24 mg, 73%); IR (neat, cm^{-1}) 2897, 2217, 1692, 1576, 1446, 1206, 804, 739, 649; ^{1}H NMR (400 MHz, $CDCl_3$) δ (ppm) 8.63 – 8.34 (m, 2H), 8.26 (dt, J = 7.1, 2.2 Hz, 2H), 7.88 – 7.40 (m, 5H). ^{13}C NMR (100 MHz, $CDCl_3$) δ (ppm) 165.7, 137.2, 132.8, 131.0, 130.8, 129.0, 127.1, 126.5, 117.3, 114.2.

2.8.1.3 Representative ^{1}H and ^{13}C NMR spectra of a selected compound

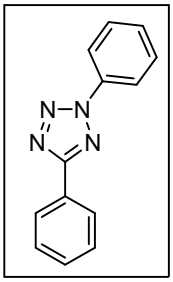

^{1}H NMR, 400 MHz, $CDCl_3$, 298 K

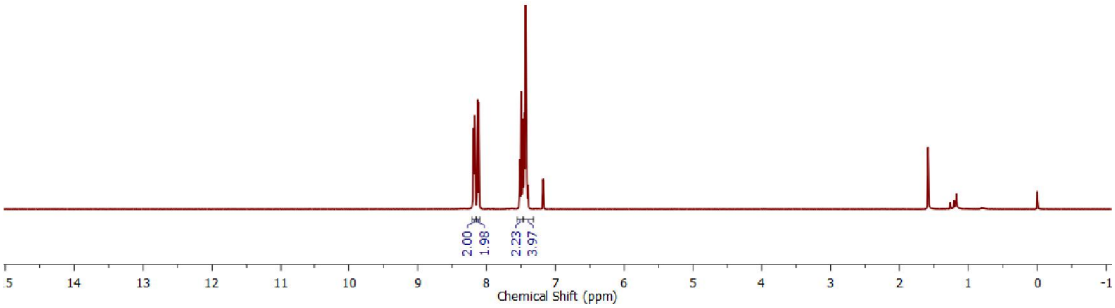

Figure **2.8** ^{1}H NMR Spectrum of **3a** in $CDCl_3$

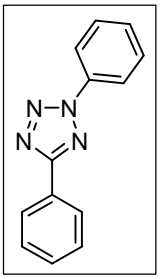

^{13}C NMR, 100 MHz, $CDCl_3$, 298 K

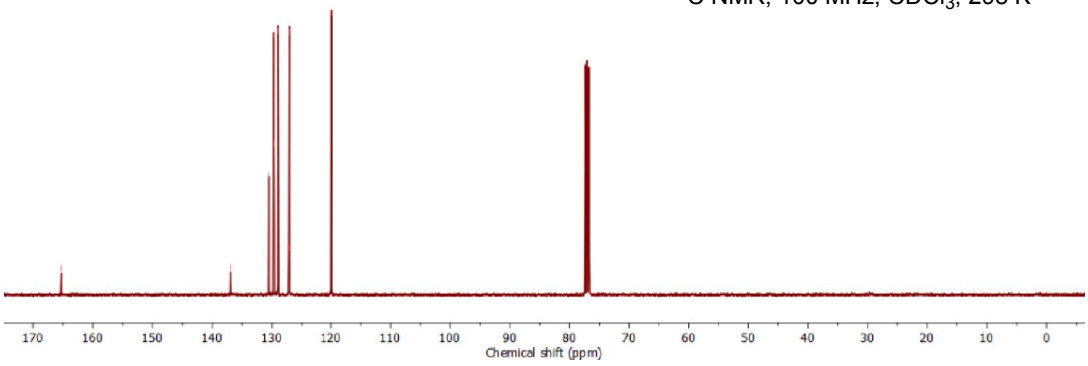

Figure **2.9** ^{13}C NMR Spectrum of **3a** in $CDCl_3$

2.9 Bibliography

[1] Rajamanickam, S., Sah, C., Mir, B. A., Ghosh, S., Sethi, G., Yadav, V., Venkataramani, S., and Patel, B. K. Bu_4NI-catalyzed, radical-induced regioselective N-alkylations and arylations of tetrazoles using organic peroxides/peresters. *The Journal of Organic Chemistry*, 85(4):2118-2141, 2020.

[2] Yang, Y.-L., Li, S., Zhang, F.-G., and Ma, J.-A. N-Iodosuccinimide-Promoted [3+2] Annulation Reaction of Aryldiazonium Salts with Guanidines To Construct Aminotetrazoles. *Organic Letters*, 23(22):8894-8898, 2021.

[3] Chen, J. Q., Li, J. H., and Dong, Z. B. A Review on the Latest Progress of Chan-Lam Coupling Reaction. *Advanced Synthesis & Catalysis*, 362(16):3311-3331, 2020.

[4] Neochoritis, C. G., Zhao, T., and Dömling, A. Tetrazoles via multicomponent reactions. *Chemical Reviews*, 119(3):1970-2042, 2019.

[5] Wang, L., Wu, W., Chen, Q., and He, M. Rhodium-catalyzed olefination of aryl tetrazoles via direct C–H bond activation. *Organic & Biomolecular Chemistry*, 12(40):7923-7926, 2014.

[6] Xiong, Q., Dong, S., Chen, Y., Liu, X., and Feng, X. Asymmetric synthesis of tetrazole and dihydroisoquinoline derivatives by isocyanide-based multicomponent reactions. *Nature Communications*, 10(1):2116, 2019.

[7] Mittal, R. and Awasthi, S. K. Recent advances in the synthesis of 5-substituted 1H-tetrazoles: A complete survey (2013–2018). *Synthesis*, 51(20):3765-3783, 2019.

[8] Reynard, G. and Lebel, H. Alkylation of 5-Substituted 1 H-Tetrazoles via the Diazotization of Aliphatic Amines. *The Journal of Organic Chemistry*, 86(17): 12452-12459, 2021.

[9] Nasrollahzadeh, M., Nezafat, Z., Bidgoli, N. S. S., and Shafiei, N. Use of tetrazoles in catalysis and energetic applications: Recent developments. *Molecular Catalysis*, 513:111788, 2021.

[10] Yahata, K., Kaneko, Y., and Akai, S. Cobalt-catalyzed hydroamination of alkenes with 5-substituted tetrazoles: facile access to 2,5-disubstituted

tetrazoles and asymmetric intermolecular hydroaminations. *Chemical and Pharmaceutical Bulletin*, 68(4):332-335, 2020.

[11] Seifried, M., Knoll, C., Giester, G., Welch, J. M., Müller, D., and Weinberger, P. Aryl and Heteroaryl N1-Tetrazoles through Ligand-Free Suzuki-Reaction under Aerobic, Aqueous Conditions. *European Journal of Organic Chemistry*, 2017(17):2416-2424, 2017.

[12] West, M. J., Fyfe, J. W., Vantourout, J. C., and Watson, A. J. Mechanistic development and recent applications of the Chan–Lam amination. *Chemical Reviews*, 119(24):12491-12523, 2019.

[13] Dhiman, N., Kaur, K., and Jaitak, V. Tetrazoles as anticancer agents: A review on synthetic strategies, mechanism of action and SAR studies. *Bioorganic & Medicinal Chemistry*, 28(15):115599, 2020.

[14] Nakamuro, T., Hagiwara, K., Miura, T., and Murakami, M. Enantioselective Denitrogenative Annulation of 1H-Tetrazoles with Styrenes Catalyzed by Rhodium. *Angewandte Chemie International Edition*, 130(19):5595-5598, 2018.

[15] Yue, T., Wang, M. X., Wang, D. X., and Zhu, J. Asymmetric synthesis of 5-(1-hydroxyalkyl) tetrazoles by catalytic enantioselective Passerini-type reactions. *Angewandte Chemie International Edition*, 47(49):9454-9457, 2008.

[16] Song, Z. J., Maligres, P., Molinaro, C., Humphrey, G., Fritzen, J., Wilson, J., and Chen, Y. Preparation of 2-(2H-Tetrazol-2-yl) benzoic Acids via Regioselective Cu (I) Catalyzed N^2 Arylation of Tetrazole. *Organic Process Research & Development*, 23(11):2354-2361, 2019.

[17] Cao, Z., Zhao, C., Zhu, J., Yan, S., Tian, L., Sun, X., and Meng, X. Gold-Catalyzed Reaction of 2H-Tetrazoles with Alkynes: Efficient Route to N-Alkenylated Tetrazoles. *ChemistrySelect*, 4(40):11785-11789, 2019.

[18] Kerru, N., Gummidi, L., Maddila, S., Gangu, K. K., and Jonnalagadda, S. B. A review on recent advances in nitrogen-containing molecules and their biological applications. *Molecules*, 25(8):1909, 2020.

[19] Roy, T., Mondal, K., Sengupta, A., and Das, P. CuF_2/MeOH-Catalyzed N^3-Selective Chan-Lam Coupling of Hydantoins: Method and Mechanistic Insight. *The Journal of Organic Chemistry*, 88(9):6058-6070, 2023.

[20] Motornov, V., Latyshev, G. V., Kotovshchikov, Y. N., Lukashev, N. V., and Beletskaya, I. P. Copper(I)-Catalyzed Regioselective Chan-Lam N^2-Vinylation of 1,2,3-Triazoles and Tetrazoles. *Advanced Synthesis & Catalysis*, 361(14): 3306-3311, 2019.

[21] Kaszás, T., Szakács, B., Juhász-Tóth, É., Cservenyák, I., Kovács, T., Juhász, L., Somsák, L., and Tóth, M. Coupling of N-Tosylhydrazones with Tetrazoles: A Regioselective Synthesis of 2,5-Disubstituted-2H-Tetrazoles. *European Journal of Organic Chemistry*, 2022(42):e202201103, 2022.

[22] Li, Y., Gao, L.-X., and Han, F.S. Efficient synthesis of 2,5-disubstituted tetrazoles via the Cu_2O-catalyzed aerobic oxidative direct cross-coupling of N–H free tetrazoles with boronic acids. *Chemical Communications*, 48(21): 2719-2721, 2012.

[23] Vishwakarma, R., Gadipelly, C., and Mannepalli, L. K. Advances in Tetrazole Synthesis–An Overview. *ChemistrySelect*, 7(29):e202200706, 2022.

[24] Behloul, C., Bouchelouche, K., Guijarro, D., Najera, C., and Yus, M. Detritylation of protected tetrazoles by naphthalene-Catalyzed lithiation. *Synthesis*, 46(15):2065-2070, 2014.

[25] Aly, A. A. and Shaker, R. M. 5-Benzyl-1H-tetrazols from the reaction of 1-aryl-5-methyl-1H-tetrazoles with 1,2-dehydrobenzene. *Tetrahedron Letters*, 46(15):2679-2682, 2005.

[26] Bladin, J. Ueber von dicyanphenylhydrazin abgeleitete verbindungen. *Berichte der deutschen chemischen Gesellschaft*, 18(1):1544-1551, 1885.

[27] Imai, T., Harigae, R., Moriyama, K., and Togo, H. Preparation of 5-Aryl-2-Alkyltetrazoles with Aromatic Aldehydes, Alkylhydrazine, Di-tert-butyl Azodicarboxylate, and [Bis(trifluoroacetoxy)iodo] benzene. *The Journal of Organic Chemistry*, 81(9):3975-3980, 2016.

[28] Bhagat, S. B. and Telvekar, V. N. L-Proline: an efficient organocatalyst for the synthesis of 5-substituted 1H-tetrazoles via [3+2] cycloaddition of nitriles and sodium azide. *Synlett*, 29(07):874-879, 2018.

[29] Kumar, S., Dubey, S., Saxena, N., and Awasthi, S. K. $(NH_4)_2Ce(NO_3)_6$ as an inexpensive, eco-friendly, efficient catalyst for the synthesis of 5-substituted 1-H tetrazoles from nitriles. *Tetrahedron Letters*, 55(44):6034-6038, 2014.

[30] Demko, Z. P. and Sharpless, K. B. Preparation of 5-substituted 1 H-tetrazoles from nitriles in water. *The Journal of Organic Chemistry*, 66(24):7945-7950, 2001.

[31] Zheng, Y. N., Zheng, H., Li, T., and Wei, W. T. Recent Advances in Copper-Catalyzed C– N Bond Formation Involving N-Centered Radicals. *ChemSusChem*, 14(24):5340-5358, 2021.

[32] Vantourout, J. C., Miras, H. N., Isidro-Llobet, A., Sproules, S., and Watson, A. J. Spectroscopic studies of the Chan–Lam amination: A mechanism-inspired solution to boronic ester reactivity. *Journal of the American Chemical Society*, 139(13):4769-4779, 2017.

[33] Yang, K., Qiu, Y., Li, Z., Wang, Z., and Jiang, S. Ligands for copper-catalyzed C–N bond forming reactions with 1 Mol% CuBr as catalyst. *The Journal of Organic Chemistry*, 76(9):3151-3159, 2011.

[34] Hardouin Duparc, V. r., Bano, G. L., and Schaper, F. Chan–Evans–Lam couplings with copper iminoarylsulfonate complexes: scope and mechanism. *ACS Catalysis*, 8(8):7308-7325, 2018.

[35] Cope, J. D., Sheridan, P. E., Galloway, C. J., Awoyemi, R. F., Stokes, S. L., and Emerson, J. P. Synthesis and characterization of a tetradentate, N-heterocyclic carbene copper (II) complex and its use as a Chan–Evans–Lam coupling catalyst. *Organometallics*, 39(24):4457-4464, 2020.

[36] Ruiz-Castillo, P. and Buchwald, S. L. Applications of palladium-catalyzed C–N cross-coupling reactions. *Chemical Reviews*, 116(19):12564-12649, 2016.

[37] Bariwal, J. and Van der Eycken, E. C–N bond forming cross-coupling reactions: an overview. *Chemical Society Reviews*, 42(24):9283-9303, 2013.

[38] Lim, C.-H., Kudisch, M., Liu, B., and Miyake, G. M. C–N cross-coupling via photoexcitation of nickel–amine complexes. *Journal of the American Chemical Society*, 140(24):7667-7673, 2018.

[39] Qiao, J. X. and Lam, P. Y. Copper-promoted carbon-heteroatom bond cross-coupling with boronic acids and derivatives. *Synthesis*, 2011(06):829-856, 2011.

[40] Rasheed, S., Rao, D. N., and Das, P. Copper-catalyzed inter-and intramolecular C–N bond formation: synthesis of benzimidazole-fused heterocycles. *The Journal of Organic Chemistry*, 80(18):9321-9327, 2015.

[41] Jia, X. and Peng, P. N, O-Bidentate ligand-tunable copper (ii) complexes as a catalyst for Chan–Lam coupling reactions of arylboronic acids with 1 H-imidazole derivatives. *Organic & Biomolecular Chemistry*, 16(46):8984-8988, 2018.

[42] Liu, Y. and Wan, J.-P. Tandem reactions initiated by copper-catalyzed cross-coupling: A new strategy towards heterocycle synthesis. *Organic & Biomolecular Chemistry*, 9(20):6873-6894, 2011.

[43] Guo, M., Li, Y., Wen, Y., and Shen, X. Synthesis of aryloxyacetamides from arylboronic acids and 2-bromoacetonitrile promoted by alkaline solutions of hydrogen peroxide. *RSC Advances*, 13(4):2631-2634, 2023.

[44] Doyle, M. G. and Lundgren, R. J. Oxidative cross-coupling processes inspired by the Chan–Lam reaction. *Chemical Communications*, 57(22):2724-2731, 2021.

[45] Vijayan, A., Rao, D. N., Radhakrishnan, K., Lam, P. Y., and Das, P. Advances in carbon–element bond construction under Chan–Lam cross-coupling conditions: a second decade. *Synthesis*, 53(05):805-847, 2021.

[46] Steemers, L., Wijsman, L., and van Maarseveen, J. H. Regio-and Stereoselective Chan-Lam-Evans Enol Esterification of Carboxylic Acids with Alkenylboroxines. *Advanced Synthesis & Catalysis*, 360(21):4241-4245, 2018.

[47] Zhuang, R., Xu, J., Cai, Z., Tang, G., Fang, M., and Zhao, Y. Copper-catalyzed C–P bond construction via direct coupling of phenylboronic acids with H-phosphonate diesters. *Organic Letters*, 13(8):2110-2113, 2011.

[48] Vyhivskyi, O., Dlin, E. A., Finko, A. V., Stepanova, S. P., Ivanenkov, Y. A., Skvortsov, D. A., Mironov, A. V., Zyk, N. V., Majouga, A. G., and Beloglazkina, E. K. Copper-Promoted C–Se Cross-Coupling of 2-Selenohydantoins with Arylboronic Acids in an Open Flask. *ACS Combinatorial Science*, 21(6):456-464, 2019.

[49] Ricordi, V. G., Freitas, C. S., Perin, G., Lenardão, E. J., Jacob, R. G., Savegnago, L., and Alves, D. Glycerol as a recyclable solvent for copper-catalyzed cross-coupling reactions of diaryl diselenides with aryl boronic acids. *Green Chemistry*, 14(4):1030-1034, 2012.

[50] Moon, P. J., Halperin, H. M., and Lundgren, R. J. Oxidative Coupling of Aryl Boron Reagents with sp^3-Carbon Nucleophiles: The Enolate Chan–Evans–

Lam Reaction. *Angewandte Chemie International Edition*, 55(5):1894-1898, 2016.

[51] Fernandes, R. A., Bhowmik, A., and Yadav, S. S. Advances in Cu and Ni-catalyzed Chan–Lam-type coupling: synthesis of diarylchalcogenides, Ar 2–X (X= S, Se, Te). *Organic & Biomolecular Chemistry*, 18(47):9583-9600, 2020.

[52] Munir, I., Zahoor, A. F., Rasool, N., Naqvi, S. A. R., Zia, K. M., and Ahmad, R. Synthetic applications and methodology development of Chan–Lam coupling: a review. *Molecular Diversity*, 23:215-259, 2019.

[53] Saikia, R., Das, S., Almin, A., Mahanta, A., Sarma, B., Thakur, A. J., and Bora, U. N, N′-Dimethylurea as an efficient ligand for the synthesis of pharma-relevant motifs through Chan–Lam cross-coupling strategy. *Organic & Biomolecular Chemistry*, 21(15):3143-3155, 2023.

[54] Saikia, R., Boruah, P. K., Ahmed, S. M., Das, M. R., Thakur, A. J., and Bora, U. An avenue to Chan-Lam N-arylation by Cu(0)nanoparticles immobilized graphitic carbon-nitride oxide surface. *Applied Catalysis A: General*, 643: 118767, 2022.

[55] Sambiagio, C., Marsden, S. P., Blacker, A. J., and McGowan, P. C. Copper catalysed Ullmann type chemistry: from mechanistic aspects to modern development. *Chemical Society Reviews*, 43(10):3525-3550, 2014.

[56] Walker, B. R., Manabe, S., Brusoe, A. T., and Sevov, C. S. Mediator-enabled electrocatalysis with ligandless copper for anaerobic Chan–Lam coupling reactions. *Journal of the American Chemical Society*, 143(16):6257-6265, 2021.

[57] Lam, P. Y., Clark, C. G., Saubern, S., Adams, J., Winters, M. P., Chan, D. M., and Combs, A. New aryl/heteroaryl C–N bond cross-coupling reactions via arylboronic acid/cupric acetate arylation. *Tetrahedron Letters*, 39(19):2941-2944, 1998.

[58] Collman, J. P. and Zhong, M. An efficient Diamine copper complex-catalyzed coupling of arylboronic acids with imidazoles. *Organic Letters*, 2(9):1233-1236, 2000.

[59] Chan, D. M., Monaco, K. L., Li, R., Bonne, D., Clark, C. G., and Lam, P. Y. Copper promoted C–N and C–O bond cross-coupling with phenyl and pyridylboronates. *Tetrahedron Letters*, 44(19):3863-3865, 2003.

[60] Onaka, T., Umemoto, H., Miki, Y., Nakamura, A., and Maegawa, T. [Cu (OH)(TMEDA)]$_2$Cl$_2$-catalyzed regioselective 2-arylation of 5-substituted tetrazoles with boronic acids under mild conditions. *The Journal of Organic Chemistry*, 79(14):6703-6707, 2014.

[61] Dar'in, D. and Krasavin, M. The Chan–Evans–Lam N-Arylation of 2-Imidazolines. *The Journal of Organic Chemistry*, 81(24):12514-12519, 2016.

[62] Guan, C., Feng, Y., Zou, G., and Tang, J. Base-assisted, copper-catalyzed N-arylation of (benz)imidazoles and amines with diarylborinic acids. *Tetrahedron*, 73(49): 6906-6913, 2017.

[63] Garnier, T., Sakly, R., Danel, M., Chassaing, S., and Pale, P. Chan–Lam-Type C–N Cross-Coupling Reactions under Base-and Ligand-Free CuI-Zeolite Catalysis. *Synthesis*, 49(06):1223-1230, 2017.

[64] Roy, S., Sarma, M. J., Kashyap, B., and Phukan, P. A quick Chan–Lam C–N and C–S cross coupling at room temperature in the presence of square pyramidal [Cu(DMAP)$_4$I]I as a catalyst. *Chemical Communications*, 52(6):1170-1173, 2016.

[65] Mondal, K., Patra, S., Halder, P., Mukhopadhyay, N., and Das, P. CuF$_2$/DMAP-Catalyzed N-Vinylation: Scope and Mechanistic Study. *Organic Letters*, 25(8): 1235-1240, 2022.